DOI: 10.35840/2631-5033/1864

VIBGYOR ePress

International Journal of
Earth Science and Geophysics

Rapid Stabilization on Global Atmospheric CO_2 Concentrations by Cheaply Enhanced Tibetan Geological Carbon Sink

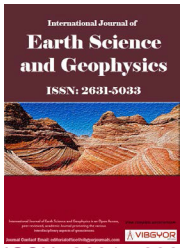

ISSN: 2631-5033

***Yan Liu*[1*], *Yanbo He*[2], *Yong Wang*[3] *and Zhongyao Gao*[4]**

[1]*Institute of Geology, Chinese Academy of Geological Sciences, Beijing 100037, China*

[2]*National Meteorological Center, China Meteorological Administration, Beijing 100081, China*

[3]*Beijing Jintu Anbang Technology Co. Ltd., Beijing 100029, China*

[4]*Geoscience Collage, Chengdu University of Technology, Chengdu 610059, China*

Abstract

Tibetan plateau is the only nascent carbon reservoir worldwide due to uniquely flat subduction of the Indian continent beneath Tibetan plateau, controlling global CO2 levels since the Oligocene. However, it remains obscure whether massive anthropogenic emissions are rapidly sequestered by the growing Tibetan plateau. Multidiscipline pieces of evidence are present here for extremely large carbon uptake during summer and relatively low carbon uptake during winter. Comprehensive investigations have further revealed that during summer, plants are highly physiological active in the tectonically active freshwater-enriched silicate regions. Huge amounts of anthropogenic emissions are thus rapidly turned into massively secondary carbonates and minor organic carbon matters by enhanced subsurface silicate chemical weathering through coupled the active tectonics and the physiologically active plant roots during summer. During winter, chemical sedimentation in salty lakes and the planting wetlands is greatly raised to transform additional anthropogenic emissions to newly-formed carbonates again, largely due to little greenhouse effect within Tibetan plateau during winter. The renascent carbonates and organic matters are subsequently buried into Tibetan thickened crust and its adjacent foreland basins by the distinguished active tectonics, and thus are hardly back to atmosphere again. More importantly, the Tibetan geological carbon sink including the enhanced subsurface silicate chemical weathering during summer and chemical sedimentation during winter, as well as the tectonic burial, can be further artificially enhanced greatly by transforming Tibetan barren deserts to planting wetlands through building simple retaining dams at the specific valleys in Tibetan plateau. The global carbon neutrality is therefore achieved cheaply quickly by the enhanced Tibetan geological carbon sink, no matter how much anthropogenic emissions in the near future.

Keywords

Cheap carbon uptake, Enhanced Tibetan geological carbon sink, Global carbon neutrality, Tibetan plateau

Introduction

Numerous studies have revealed that rates of carbon uptake by well-known land carbon reservoirs such as African [1] and Amazonian [2] tropical forests, and ecosystem of Chinese mainland [3], as well as ocean carbon reservoirs

***Corresponding author:** *Yan Liu, Institute of Geology, Chinese Academy of Geological Sciences, Beijing 100037, China, Tel: +86-13683312011*

Accepted: February 13, 2023; **Published:** February 15, 2023

Citation: Liu Y, He Y, Wang Y, Gao Z (2023) Rapid Stabilization on Global Atmospheric CO_2 Concentrations by Cheaply Enhanced Tibetan Geological Carbon Sink. Int J Earth Sci Geophys 9:064

[4,5] have remained constant or declined in recent decades [6], leading to severe consequences such as serious shortage of food and freshwater around the North Atlantic. Consequently, fast and cheap removal of massive anthropogenic emissions is an urgent need worldwide today. Several expensive approaches have been used to try to stabilize global atmospheric CO_2 concentrations [7]. For example, the CO_2 gas with high concentrations from condensed flue gas or other enriched sources have been subsequently injected into deep regions, particularly into deep oil reservoirs [7]. A large amount of silicate powder is scattered to croplands [8], grasslands and forests as an alternative approach to try to remove atmospheric CO_2 [7]. Unfortunately, these approaches normally require relatively high energy and infrastructure inputs every year [8]. And hence, much work has been done and much money has been spent [7,8], the global atmospheric CO_2 concentrations still remain relatively high growth rates. This means that these expensive approaches do not work well, largely due to the fact that it is still little-known what mechanisms are really responsible for rapidly net uptake of global atmospheric CO_2 [6,9,10], despite it has been well known for a long time that negative carbon-climate feedbacks stabilized Earth's long-term climate [11-13] and, in particular, atmospheric CO_2 levels [6,9,10].

In-depth understanding of the mechanisms controlling the historically changing processes of atmospheric CO_2 concentrations is, no doubt, critical to cheaply achieve global carbon neutrality in the near future. Numerous studies have previously revealed that during the Eocene, the atmospheric CO_2 concentrations were approximately 5 times that for today [14,15]. During the Eocene-Oligocene transition, the global atmospheric CO_2 concentrations plummeted quickly, leading to the formation of the Antarctic ice sheets [16,17]. However, it still remains controversial where the huge amounts of atmospheric CO_2 sink [6,14,18,19]. From a global mass balance perspective, it clearly suggests that at least one unknown carbon reservoir has continuously accommodated the huge amounts of atmospheric CO_2 since the late Eocene.

The persistent convergence between Indian and Asian continents has created growing Tibetan plateau (Figure 1). Gravity isostasy suggests that

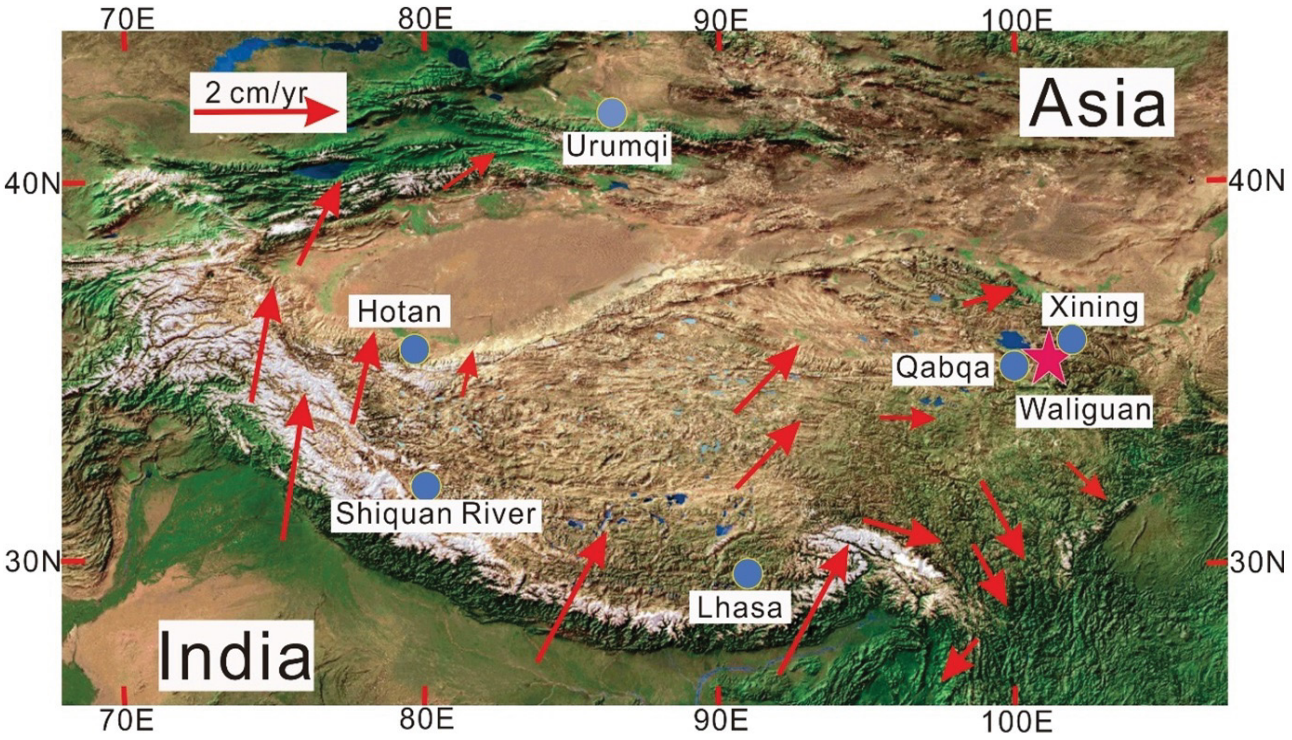

Figure 1: Sketch map showing meteorological stations and crustal horizontal shortening direction and rates [34] (red arrow) in the studying region. Barren deserts are yellow and/or brown yellow regions. Salty lakes are small irregular light blue or blue areas within the yellow and/or brown yellow regions. Green regions are covered by various plants. White areas are covered by snow and/or ice sheets.

ISSN: 2631-5033

Citation: Liu Y, He Y, Wang Y, Gao Z (2023) Rapid Stabilization on Global Atmospheric CO_2 Concentrations by Cheaply Enhanced Tibetan Geological Carbon Sink. Int J Earth Sci Geophys 9:064

Table 1: Monthly mean precipitation in millimeters (P), temperature in °C (T), and Waliguan atmospheric CO_2 concentrations in ppmv.

		Waliguan	Lhasa		Shiquanhe		Xining		Qabqa		Hotan		Urumqi	
year	month	CO_2	P	T	P	T	P	T	P	T	P	T	P	T
1990	8	349.01	145.6	14.1	30.4	13.7	50.2	17.2	40	15.3	0	25.4	4.4	22.6
1990	9	351.55	90	12.4	3.7	10.2	29	13.6	26.9	11	0	20.8	13.1	17.6
1990	10	353.88	5.9	8.5	0	0.1	16.8	7.5	30.8	4.2	0	12.5	16.2	9.6
1990	11	354.64	0	3.4	0.2	-6.1	3.2	2.1	0.8	-1.6	0	5.7	43.1	-1.8
1990	12	355.63	0	-1.2	0.9	-9.1	0.3	-3.9	1	-7.3	2	-3.3	6.9	-7.2
1991	1	357.21	1.8	-2.9	0.4	-15.8	3.4	-6.7	2.9	-9.9	0.4	-4.9	5.1	-11.2
1991	2	358.31	1.8	2.9	0.1	-9.2	1	-2.3	1	-4.8	0.5	-0.6	6.5	-10.3
1991	3	359.65	0	6.1	0.3	-4.5	1.9	3.3	1.5	1.6	0.1	9.3	17.7	-2.9
1991	4	360.95	9.3	9.3	0.4	-1.5	14	7.9	23.1	5.5	2.7	15.4	1.3	10.7
1991	5	360.20	40	12.8	2.5	4.2	34.6	12.5	30	10.7	4.5	19.9	8.7	18.3
1991	6	354.78	77.3	15.4	2	10.6	50	16.7	60	15	999999	23.7	999999	22.2
1991	7	347.53	151.6	15.9	0.1	15.7	77.8	19	80.8	16.7	999999	24.7	999999	24.6
1991	8	347.81	145.1	14.4	21.1	13.3	34.2	18.5	70	15.6	21.2	22.6	999999	21.9
1991	9	353.05	77.1	12.8	10	9.6	13.4	13.4	6.5	10.8	0	20.6	8.8	18.1
1991	10	355.05	0	9.6	0	-0.1	13.4	7.4	8	5.1	0	11.7	9.2	9.8
1991	11	355.44	0.3	2.4	0	-6.4	0.3	-0.8	0	-4.5	0	3.8	4.3	-0.9
1991	12	355.83	0.6	-2	0.2	-9.9	1.4	-5.3	1.3	-8.6	999999	-1.4	999999	-8.5
1992	1	357.83	1.4	-2.2	1.3	-9.5	0	-6.5	0	-10.2	1.1	-4.2	9.6	-9.4
1992	2	359.06	1.1	-0.6	2.9	-11.5	0.3	-4.5	0.1	-7.6	0.4	1.5	999999	-8
1992	3	360.08	3.2	7	3.3	-5.4	1	2	13.4	0	3.7	7.4	18.2	-0.8
1992	4	362.13	2.6	8.8	0	-0.2	15.2	9.6	5.8	7.4	0	18.1	31.1	11.4
1992	5	361.86	30.8	11.2	1	3.2	82.9	12	48.5	10.6	19.2	19.2	68.7	15.8
1992	6	356.22	40.6	16.6	2.4	8.7	999999	16	57.1	13.6	28.3	22.7	30.4	21.3
1992	7	352.64	67	16.3	5	12.1	89.1	16.6	76.7	13.7	0.6	25.4	73.5	22.7
1992	8	352.43	91	15.1	10	14.2	999999	16.7	55.9	15.1	6	23.5	7.8	20.3
1992	9	353.46	42.8	13.8	0.3	9.2	106.7	12.6	65.6	10.8	2.4	19.5	37.4	12
1992	10	355.14	4.3	8.8	0	0.6	28	5.6	24.3	3.1	0	11.3	16.3	6.3

1992	11	355.62	0.4	2	1.3	-6.1	3.5	-0.1	2.2	-3.7	0	4.3	24.1	-2.9
1992	12	357.06	6.5	-3.9	0	-10	1	-3.7	0.7	-7.1	0	-0.6	10	-8.5
1993	1	359.48	1.3	0.1	0.7	-10.1	2	-8.2	3.6	-10.9	5.2	-4.7	3.2	-12.4
1993	2	359.35	0.1	1.6	1.2	-6.9	7.3	-1	3.7	-3.2	5.7	3.2	22.7	-7.2
1993	3	359.71	7.7	4.8	1.1	-7.3	5.2	3.6	22.2	1.1	9.9	8.7	34.4	0.2
1993	4	361.19	7.4	8.3	0	-0.4	2.1	9.3	0	6.7	0	17.8	15.8	9
1993	5	361.21	15.3	12.3	0	5.6	116.5	10.7	81.8	9.1	7.6	19.2	36.8	14.2
1993	6	357.95	67.8	15	7.6	10.9	42.7	15.1	59.3	12.8	5	23.9	52.6	20.9
1993	7	353.23	149.2	16.4	1.8	14.6	93.5	16.8	98.7	15.1	6.1	24.7	29.7	22.9
1993	8	352.14	139.6	15.3	0	14.1	88.3	15.9	58.4	14.1	28.7	22.3	40.3	20.6
1993	9	355.93	147.2	12.3	43.7	8	52.8	12.4	59.8	10.1	0	20.6	25.4	15.5
1993	10	357.47	1.2	9.6	0	1	11.2	6.5	10	3.6	0	11.1	10	7.3
1993	11	356.93	0.4	3	0	-4.3	0	1	0	-1.1	0.8	3.8	12	-5.3
1993	12	357.44	0	-0.4	0	-9.1	0	-4.6	0	-6.8	0	-2.8	17.7	-12.1
1994	1	359.11	0.1	0.8	2.4	-11.3	0.9	-6.3	2.8	-8.3	2.7	-4	9	-12.5
1994	2	361.39	0	1.3	1.1	-10.7	0.3	-1.7	0	-4.3	0	1.6	10	-11.7
1994	3	363.10	5	4.6	0.5	-4	2.2	1.7	0	-0.5	0	9	8.8	-3
1994	4	363.84	4.8	8.8	0	-1.6	19.4	9.6	16.7	7	0.4	15.3	77.8	8.3
1994	5	363.06	31.9	13	1.5	4.7	17.5	13.6	40.6	10.9	0	21.3	24.2	16.7
1994	6	359.66	50.5	16.4	0	11.3	110.4	15.7	63.9	13.8	7.5	24.8	18.9	21.4
1994	7	355.63	96.8	17	5	14.5	106.2	17.6	75.3	15.6	0	27.7	39.1	24
1994	8	355.09	70.2	15.6	6	13.6	87.7	17.8	999999	16.2	3.5	25.7	3.8	22.9
1994	9	356.80	111.6	13.8	0	9.9	999999	12.8	999999	11.7	0	18.9	19.4	14.5
1994	10	358.19	0.2	9.1	0	0.3	999999	6	4	3.7	0	11.9	48.2	6.1
1996	9	360.37	66.3	13	8.9	9.3	34.9	12	38	11	0	20.5	19.7	17.4
1996	10	361.06	6.6	10	0.7	0.5	15.8	5.6	14.9	4.7	9	12.5	33.8	8.2
1996	11	361.67	0	4.6	0	-4.4	3.1	-1.6	0	-3.1	0	4.6	25.7	-2.4
1996	12	362.90	0	-0.7	0	-8.8	0	-7.3	0	-9.6	0	-1.3	9.2	-7
1997	1	364.93	3.7	-2.8	0	-12.2	0.5	-6.3	1.1	-8.1	0	-1.3	9.7	-10.4
1997	2	366.52	0	1.4	0	-10.4	1.2	-4.5	4.6	-6.8	0	1.8	3.6	-9.3

Citation: Liu Y, He Y, Wang Y, Gao Z (2023) Rapid Stabilization on Global Atmospheric CO_2 Concentrations by Cheaply Enhanced Tibetan Geological Carbon Sink. Int J Earth Sci Geophys 9:064

ISSN: 2631-5033

1997	3	367.64	5	5	2.4	-4.3	25.9	3.6	4.4	1.6	0	10.5	13	2.9
1997	4	368.74	10	6.1	0.1	0.3	54.3	6.8	13	5.6	0	18.4	0.2	16.3
1997	5	367.35	18.6	12.2	0.9	3.6	999999	12.8	999999	11.1	0.6	21.7	45.1	19.2
1997	6	362.90	40	14.8	3.2	10.4	999999	15	999999	13.6	999999	24.5	11.5	22.9
1997	7	358.92	58.7	16.3	13.1	15	999999	16.8	65.8	16	1.3	27.5	20.2	24.4
1997	8	358.69	47.9	15.7	8	13.4	105.2	15.9	80.6	15.7	2	24.3	21.1	23.3
1997	9	361.11	88.8	12.3	1	10.2	41.3	10.5	39.7	9.5	0	20.8	0.6	19.3
1997	10	363.20	2.8	6.7	16.3	-1	5.1	5.1	0	4.4	0	13.7	0.2	12.7
1997	11	364.24	1.3	3.2	1.1	-6.4	8.9	-2.4	5.1	-3.1	0	4.2	27.4	-4.5
1997	12	364.87	0.3	-0.6	999999	-17	0.9	-7	0	-7.9	0	-3.6	7.2	-10.8
1998	1	366.54	0	-0.2	0.2	-14.4	4	-10.1	1.1	-9.4	1.8	-4.4	6.8	-13.5
1998	2	367.66	0.1	2.6	0.7	-8.8	0.5	-1.8	0.2	-2.6	0	3.2	10.8	-5.8
1998	3	368.16	19.3	4.3	2.3	-5.9	23	1.1	14.2	0.3	9.4	8.1	18	-1.7
1998	4	370.12	14.3	8	0	0.9	30.4	11.5	5.8	10.1	0	18.4	56.1	9.7
1998	5	368.99	11.3	14	0.1	6	82.3	12.5	42	12.5	0	20.8	126.1	15.1
1998	6	363.07	85.7	18.2	3.8	10.8	79.6	15.7	999999	16	999999	24.2	9.1	23.2
1998	7	359.88	144.6	16	4.5	16	79.8	17.1	106.4	15.8	999999	26.5	73.9	23.5
1998	8	361.42	226.2	14.9	30	15.2	105.9	15.6	61.1	14.7	999999	24.2	56.1	23.6
1998	9	364.38	63.2	14	40	11.1	50	12.8	17.7	12.8	0.1	21.5	18.5	17.6
1998	10	365.57	16.2	11.5	24.5	0.9	28.4	6.3	9	6	0	13.7	9	8.9
1998	11	366.76	0	5.1	0	-7.7	0	0.2	0	-1.7	0	7	14.6	1
1998	12	368.59	0	-0.3	0	-11.1	0.6	-5	0.8	-6.6	1.4	0.3	999999	-7.7
1999	1	369.69	0	-1.3	0.5	-10.6	0	-7.4	0.3	-8.5	2.3	-3.1	20	-11.6
1999	2	370.80	6.2	4	2.3	-7.4	0	-3	1.2	-2.9	0	3.1	2.4	-5.9
1999	3	371.48	1.1	7.5	0.2	-3.9	5.2	2.4	3.1	1.9	0.2	10.3	29.9	-3
1999	4	372.78	0.3	12.7	1.5	1	3.7	8.5	0	7.7	3.7	16.2	23.8	10.8
1999	5	372.89	40	13.6	2	6.9	50	12.2	28.4	10.6	0	22.1	20.6	18.3
1999	6	367.90	75.4	17	2.6	10.9	105.6	15.2	50	14.1	0	25.3	48.4	21.5
1999	7	362.48	130.9	15.6	35.7	14.9	78.3	17	72.6	15.5	6.8	25.2	27.6	24.4
1999	8	362.64	160.1	14.5	66.7	12.8	94.5	16.2	86.7	15.2	19.3	25.3	60.9	22.5

Citation: Liu Y, He Y, Wang Y, Gao Z (2023) Rapid Stabilization on Global Atmospheric CO_2 Concentrations by Cheaply Enhanced Tibetan Geological Carbon Sink. Int J Earth Sci Geophys 9:064

ISSN: 2631-5033

1999	9	365.87	95.9	13	6.5	10.8	50	12.7	41.7	11.9	0	22.6	33.2	16.9
1999	10	367.21	5.1	10.4	0	1.6	43	6.2	19	5.6	0	14.2	23.1	10.3
1999	11	368.46	0	4.1	0	-3.7	4.5	-0.1	2.2	-0.6	0	4.9	13.7	-1.5
1999	12	369.20	0	-0.7	0	-8.5	1.1	-6.3	0	-7.9	0	-0.3	32.8	-7
2000	1	369.99	3.5	-0.5	0	-9.7	1.6	-7.1	0.1	-7.3	0.1	-1.3	25	-13.9
2000	2	372.25	0.1	1.8	3.5	-13.3	4.2	-6	0.5	-6.7	0	0.4	20.6	-9.5
2000	3	374.59	9.2	4.6	0.4	-6.2	3.5	1.6	4.3	0	0	9.3	13.7	-0.5
2000	4	374.58	8.9	9.1	1.5	0.6	17.1	7.5	1.7	5.9	1	18	20.6	13.2
2000	5	372.75	39.9	12.5	12.6	8.4	20	13.6	6.2	12.6	7.7	24.1	25.5	19.1
2000	6	370.54	60.2	17.2	25	12.1	30	15.2	10	14.8	7.7	24.7	58.2	21.9
2000	7	366.58	170.4	15.1	66	14.2	46.9	19.7	30	19.4	1.9	25.8	19.1	24.7
2000	8	365.52	164.5	14.1	4.9	13.7	62.2	15.6	20	15.1	0	25.5	42.1	23
2000	9	368.20	71.3	12.9	1	9.7	87.7	11.2	10	10.5	0.2	20.4	16.2	17.8
2000	10	369.71	1.7	9.4	0	2	21.7	5.8	6.4	5.9	0	13.5	49.8	3.1
2000	11	370.13	0	4.6	0.9	-3.9	17.7	-2.3	8.4	-2.7	0	4.9	27.6	-4.8
2000	12	371.44	0	-0.2	0	-8.4	1.2	-5.8	0.9	-7.2	0.6	-2.7	8.6	-7
2001	1	372.82	0	1.1	3.5	-10	0.9	-6.9	1	-7.8	0	-3.3	25.9	-11.8
2001	2	373.34	0.8	4.7	1.3	-7.1	0.7	-3.3	0.4	-3.9	0	2.5	7	-8.9
2001	3	374.70	0.4	4.9	0.8	-4.8	0	1.6	0	0.2	0	10.9	4.2	3
2001	4	376.43	6.2	8.1	0.1	1.1	8.1	7.4	12.1	6.2	0.1	17	47.1	9.7
2001	5	374.91	55	12.4	1	7.4	36.3	11.6	36.5	9.7	3.5	22.9	6.1	19.9
2001	6	371.23	150.6	14.6	8	12.7	48.7	15.6	37.5	14.5	0.3	25.9	21.9	23.1
2001	7	366.37	143.6	15.9	20	15.8	110.8	17.6	120	17.7	11	26.3	61.7	23.4
2001	8	363.36	82	15.4	10	15	65.5	15.6	78.3	15	4	24.6	12.8	23.4
2001	9	367.51	40.2	14.3	0	8.9	119.3	12.4	69	11.7	0	20.8	35.7	16.2
2001	10	372.96	13.5	9.2	0	2.2	5.8	7.3	1.8	6.1	2.8	14.2	41.3	8
2001	11	372.72	0	3.9	0	-5.2	1.6	0.1	0.5	-1.1	0.3	6.5	8.5	1.7
2001	12	372.42	0	1	0.3	-8.9	0.1	-6.6	1.3	-7	4	-3.2	999999	-15.2
2002	1	374.36	0.4	-0.5	0.3	-12.5	6.4	-7.8	3.3	-9.4	9.6	-5.5	9.6	-9
2002	2	374.98	0.9	3.6	3.7	-9.7	0.2	-2.6	0	-3.8	0	0.7	16.6	-6.9

Citation: Liu Y, He Y, Wang Y, Gao Z (2023) Rapid Stabilization on Global Atmospheric CO_2 Concentrations by Cheaply Enhanced Tibetan Geological Carbon Sink. Int J Earth Sci Geophys 9:064

2002	3	375.50	2.3	5.6	2	-5.9	9.9	2.8	2.6	1.5	0	12.1	33.2	0.7
2002	4	377.16	999999	8.6	4.7	1	47.1	8.5	28.6	8.4	1.5	17.2	90.2	7.8
2002	5	377.01	999999	11.4	0	5.1	999999	11	60.6	9.3	0.4	21.9	20.4	17.3
2002	6	372.02	79.3	16.6	11.3	11.2	999999	16.2	999999	15.1	3.3	26.1	62.1	21.9
2002	7	366.20	163.5	16.1	0.1	15.4	41.9	17.8	55.3	16.6	25.1	23.9	38.3	23.5
2002	8	366.25	137.9	15.1	70.8	12.9	73.7	16.6	999999	15.5	0	26.9	4.6	24.7
2002	9	370.15	94.2	13.2	11	7.5	999999	11.9	47	11	18.2	18.7	15.8	17.5
2002	10	372.21	6.1	8.7	0.4	0.5	20.8	5.6	0.6	4.8	0	15.6	7.9	9.9
2002	11	373.18	0	4.2	0.3	-5.4	7.9	-1.6	2.9	-2.9	0	7	16.1	1.6
2002	12	374.80	0	0.5	0.2	-7.8	0.5	-6.9	0	-7	5.7	-3.5	28.1	-11.8
2003	1	376.07	1.3	-0.4	1.5	-11.2	0.2	-6.7	0	-8.6	0	-2.6	13.3	-10.5
2003	2	377.27	2.9	1.4	2.6	-9.3	0	-2.5	0	-3.2	0.5	2.6	999999	-8.5
2003	3	378.20	2.9	5.3	0	-4.7	999999	2.2	3.8	1.4	9.4	9.3	11.6	-2.1
2003	4	379.38	2.6	9.4	3.5	0.8	35.9	8.2	999999	7.8	6.2	15.9	38.1	7
2003	5	379.71	999999	11.6	0.1	2.8	78.4	11.7	34.9	10.6	20.7	19.8	59.2	15.5
2003	6	375.94	192.5	14.3	0.8	11.3	999999	14.7	999999	14.3	25.6	24.2	35.2	22.8
2003	7	372.29	93.1	15.8	999999	14.9	122.4	16.5	62	15.9	1.2	27.7	68.7	21.1
2003	8	372.68	124.1	17	20.5	15.1	108.3	16.3	999999	15.9	8.3	24.1	48.3	22
2003	9	374.66	95.3	14.1	0.8	10.8	54.4	12.3	42	11.9	6.6	20.7	52.1	17.2
2003	10	375.76	3.3	10.9	0	0.4	27.5	5.8	9.2	4.6	4.9	13.7	0.1	10.1
2003	11	376.68	0	5.1	0	-5	5.6	-0.4	0	-1.1	2.7	6.3	27	-3.2
2003	12	378.15	0	0.6	0.1	-9.8	3.4	-6.8	5.6	-7.6	0	-1.6	999999	-10.2
2004	1	378.85	0.2	-0.9	0.1	-10.4	2.1	-8.4	999999	-10.8	1.3	-3.4	9.6	-12.6
2004	2	379.92	1.7	1.3	0	-8.5	5.3	-3.7	2.5	-5.3	0.2	3.4	37.6	-6.9
2004	3	382.25	0.2	8.4	0	-1.8	6	2.9	5	2.6	9	12.2	24.3	0.4
2004	4	383.61	26.2	7.9	0.1	2.9	19.7	9.5	18.2	7.9	5.6	18.5	23.1	13.4
2004	5	380.07	56.9	14	0	6.3	69	11.2	46.3	9.9	14	20.6	36.5	18
2004	6	374.55	180	15.5	13.6	10.6	999999	14.9	80.9	13.8	7.2	24.8	6.4	22.7
2004	7	374.67	227.6	14.3	5.2	15	61.3	16.6	73.8	15.3	0	26.9	59.6	24.7
2004	8	374.52	118	15.7	11.3	13.5	999999	16.5	999999	15.9	3	24.8	26.8	22

Citation: Liu Y, He Y, Wang Y, Gao Z (2023) Rapid Stabilization on Global Atmospheric CO_2 Concentrations by Cheaply Enhanced Tibetan Geological Carbon Sink. Int J Earth Sci Geophys 9:064

ISSN: 2631-5033

2004	9	374.36	32.4	14.3	0	10	99.6	11.1	999999	10.9	0	21.6	14.3	16.2
2004	10	377.90	9	8.6	1.6	0.2	999999	5.6	24	4.4	0	13.3	14.8	7.6
2004	11	379.24	4.1	2.6	0	-5.9	1.1	-1.5	0	-2.9	0	7.2	17.2	-1.4
2004	12	380.24	0	0.4	3.7	-8	7.3	-5.5	1	-6.4	0	-0.3	44	-8.3
2005	1	383.59	4.1	-0.1	0.5	-15.3	1.7	-7.8	0.9	-7.3	0.5	-2.6	5.6	-14.7
2005	2	384.29	999999	3.8	0.3	-8.5	6.2	-4.4	3.7	-3.6	1.7	-0.2	4	-14.8
2005	3	383.69	1.2	6.7	0	-3.6	19.1	1.7	9.6	1.3	0.6	11.5	6.5	2.4
2005	4	384.75	7.7	9.4	0.8	-0.9	8.5	8.2	28.3	6.3	29.8	16.9	35.2	11.8
2005	5	384.08	29.5	11	1.2	3.8	999999	12.6	999999	11	19.8	20	25	17.7
2005	6	380.52	999999	17.2	5.4	9.9	79.7	15.8	55	14.3	3.7	25.5	28.6	23.2
2005	7	375.83	999999	17.6	999999	15.1	106.8	17.2	78.4	15.9	16.7	25.5	16.7	25.5
2005	8	373.57	167.2	16.3	4.1	14.7	106.3	16.7	83.4	15.6	9.3	23.8	86.7	21.5
2005	9	376.25	75.5	14.6	17.7	10.5	66.5	12.8	53.6	11.8	6.3	22.5	2	19
2005	10	379.59	21.1	9.7	0	1.2	26	5.6	14.6	4.8	999999	14.1	9	9.7
2005	11	379.91	0	4.3	0.1	-5.8	1.6	-0.9	3.7	-2.4	999999	5.7	33.1	-0.1
2005	12	380.94	999999	0.5	0.2	-10.4	0	-8.2	0	-7	0	-3.5	23.9	-10.8
2006	1	382.78	999999	2.7	4	-8.5	1.8	-6.5	1.4	-5.6	6	-8.4	17.3	-14.2
2006	2	383.46	0	5	0.7	-4.4	6.1	-3.1	1.9	-2.4	7.6	1.6	43.1	-6.7
2006	3	385.23	0.8	6.2	0	-4.3	1.7	1.4	0	0.6	999999	10.2	10.2	1.2
2006	4	387.08	999999	8.3	999999	0	15.6	7.2	20.4	5.2	3.9	17.4	19.3	12
2006	5	385.49	999999	12.8	3.9	8.7	48.7	12	27.5	11.2	1	23.2	50.7	16.8
2006	6	381.44	999999	17.8	1.3	10.5	53.3	15.5	61.1	13.9	5.2	24.4	16.3	23.2
2006	7	377.87	999999	18.3	27	15.1	55.8	18.7	76.2	18.2	16.8	26.4	12.2	24.5
2006	8	377.81	999999	17.1	49.4	13.5	61.9	18.3	60.2	17.3	0	27.2	7.2	24.2
2006	9	379.70	999999	14.7	0	10.2	78.8	11.7	76.2	11.3	0	21.8	7.4	17.6
2006	10	381.20	999999	8.6	5.2	1.7	999999	7.6	0.9	6.5	0	17.6	15.5	11.4
2006	11	381.86	1.3	3.7	0.1	-4.4	6.6	0.3	1.5	-1	1.2	7.4	31.1	1.9
2006	12	383.59	0.1	1.3	0.1	-8.8	4	-6.4	4.8	-7.6	999999	-1.7	5.6	-8.8
2007	1	384.98	999999	2.5	999999	-9.6	2.9	-8.6	0.7	-8.7	999999	-2.4	17.2	-10.4
2007	2	385.75	0.7	0.9	0.2	-7.6	1.5	-2.2	4.7	-4.1	0	5.9	11	-5

Citation: Liu Y, He Y, Wang Y, Gao Z (2023) Rapid Stabilization on Global Atmospheric CO_2 Concentrations by Cheaply Enhanced Tibetan Geological Carbon Sink. Int J Earth Sci Geophys 9:064

ISSN: 2631-5033

2007	3	387.48	2.4	7.1	2.6	-5.1	999999	2.3	12.3	1.8	6.3	10.8	7.6	0.4
2007	4	389.12	26.2	9.4	3	3.1	18.1	7.3	0.6	7.3	0	20.1	33.3	13.6
2007	5	387.54	7.1	15.6	999999	6.4	38.6	14.3	21.3	13.2	1.1	23.7	107.7	16.4
2007	6	385.46	63.1	16.2	0.1	12.6	92.7	15	999999	13.3	5.3	26.3	16.8	22.4
2007	7	381.68	155.6	17.5	999999	15.7	73.9	16.7	62	15.9	2.1	26.8	107.6	23.9
2007	8	377.76	168.9	16.3	9.3	14.8	175.6	17.2	80.5	17	0	25.8	53.5	22.1
2007	9	380.54	50.7	14.5	4.5	10.6	53.7	11.6	32.4	11.1	8.9	20.8	27.1	18.6
2007	10	383.32	0.7	12.1	0	0.9	39.5	5.5	43.4	5.3	0	13.1	15.3	7.8
2007	11	383.65	1.9	4	0	-5.4	3.2	-0.5	999999	-1.6	999999	7	5.4	1
2007	12	385.80	0	1	0	-8.1	1.8	-5.4	0.3	-6.1	0.1	-0.7	17	-9
2008	1	387.66	0.2	1.6	3.7	-10.8	2.6	-9.6	4.9	-8.9	7	-8.5	3	-15.6
2008	2	388.24	7.5	1.4	0	-9.9	2.7	-7.9	5.2	-8.2	16.5	-5.6	11.6	-9.6
2008	3	389.78	3.8	5.6	1.3	-4.2	7.7	3.4	4	2.1	0.6	13.8	17.8	5.2
2008	4	391.06	3.8	10.2	0.4	0.4	32.2	8.3	9.9	7.6	999999	17	21.7	11.1
2008	5	389.42	999999	13.5	18.9	5.5	48.4	13.3	25	12.8	5	23.2	15.8	20.7
2008	6	384.84	63	15.9	8.6	13.8	999999	14.8	49.2	13.6	0.1	27.3	8.9	24.1
2008	7	381.34	162.3	16.3	10	15.5	41.6	17.9	84.6	16.4	4.9	26.6	20.9	25.2
2008	8	381.51	161.9	15	999999	13.4	99.7	15.4	79.3	14.4	0	26.8	17.1	23.5
2008	9	383.71	49.4	14.4	11.3	7.3	62.9	12.5	85.4	12	0	21.8	16.8	17
2008	10	385.48	10.9	8.9	0	0.2	19.7	7	999999	5.9	0	14.7	12.8	10.1
2008	11	386.29	6.9	3.9	0	-3.9	0.2	-0.3	2.6	-1.6	0	6	12.8	0.9
2008	12	386.77	0	1	0	-7.7	0	-5.9	999999	-5.9	0.2	-0.2	12.6	-8.2
2009	1	387.65	0	1	0.2	-8.8	4.7	-7.8	0.3	-7.1	0	-2.1	6.3	-9.9
2009	2	388.83	0.6	3.8	0.6	-7.5	0.4	-0.8	1.8	-2	0.8	4.8	11.8	-8.8
2009	3	391.04	5.2	5.8	0	-3.7	15.7	2	2.6	1.5	0	12.1	35	2.5
2009	4	393.24	0.8	11.5	0	1.1	18.4	9.8	999999	8.8	0.1	18.7	65.1	13
2009	5	391.15	1.1	14.2	5.4	4.8	66.4	12.1	54.7	10.5	0.5	21.6	70.9	16.1
2009	6	385.79	37.9	18.6	0	10.2	66.7	15.8	999999	15.2	1.1	25.4	39.3	20.8
2009	7	383.07	999999	19.6	5.4	14.6	68.2	17.8	999999	16.6	0.9	26.9	10.8	23.7
2009	8	381.95	191.4	16.4	0.8	15	106.5	15.4	85.3	14.7	0	26.5	12.4	22.9

Citation: Liu Y, He Y, Wang Y, Gao Z (2023) Rapid Stabilization on Global Atmospheric CO_2 Concentrations by Cheaply Enhanced Tibetan Geological Carbon Sink. Int J Earth Sci Geophys 9:064

2009	9	383.96	999999	15	12.9	8	87.3	13.1	78.9	12.4	8.9	21.4	35.3	16.8
2009	10	387.38	8	11.2	0	0.6	16.9	5.9	10.4	4.9	0	15.6	15.5	10.9
2009	11	388.28	0	5.7	0	-4.9	7.1	-2.2	2.2	-2	6.9	4.2	27.5	-2.3
2009	12	388.73	0.1	0.5	0	-9.3	0.8	-6.4	0	-6.6	0	0.1	23.2	-10
2010	1	390.34	0	-0.5	5.9	-15.4	1.2	-5.6	0	-5.4	0	-0.5	15.6	-10.6
2010	2	392.16	0.1	3.3	1.5	-8.6	1.2	-3.2	0.8	-2.5	11.3	1.8	9.5	-12.4
2010	3	393.25	2.9	8	0	-1.7	4.2	2.5	0.1	2.5	15.8	11.8	46.8	-4.4
2010	4	394.48	999999	11.4	0.2	2.4	17.6	7.2	7.8	7.2	0	17.3	30	8.7
2010	5	393.10	999999	14.3	0	6.1	99	12.4	48.8	11.9	23.5	21	26.2	16.2
2010	6	388.86	35.2	18.8	1.2	9.9	999999	15.4	90	13.8	31.5	22.3	31.2	22.5
2010	7	386.77	999999	18	26.8	14.4	58.2	18.8	999999	17.9	2.8	26.3	13.2	24
2010	8	385.90	142.7	16.5	50.8	14.1	65.4	17.5	82.6	17	0.3	27.4	12.5	22.8
2010	9	387.77	70.1	14.5	3.8	10.7	72.6	13.5	31.4	13.2	13.3	20.2	5.1	18
2010	10	389.57	999999	10	0	1.6	33.2	6	7.8	5.1	13.4	14.6	32.5	9.7
2010	11	389.54	0	5.7	0	-4.1	0.4	-0.9	0	-2.4	0	7.6	28.3	2.4
2010	12	391.19	0	-0.3	0.9	-9.9	1.2	-7.3	0.9	-8.3	0	-0.7	31.5	-8.2
2011	1	393.23	0	0.2	0.5	-13.7	1	-11.2	0	-9.4	0	-6.8	11	-18.8
2011	2	394.01	0	2.5	2.2	-8.7	0.4	-2.7	0.4	-2.3	0.6	2.6	17.2	-8.7
2011	3	395.56	1	6.2	0.1	-4.1	2.1	-1.3	0.2	-1	0	7.1	20.1	-5.2
2011	4	397.28	2.2	9.6	0.4	0.4	7.1	9	17.2	7.5	0	18.6	46.6	13.2
2011	5	396.24	37.1	13.4	3.3	7	49.5	11.9	44.8	10.8	4.4	23.3	43.5	17.1
2011	6	391.14	999999	17	11.6	11.5	63.4	16.5	72.2	14.6	0.3	26.3	22.4	23.1
2011	7	385.92	198.6	16.2	23.3	15.3	54.5	16.8	63.5	15.8	0.2	27.1	64.9	24.6
2011	8	386.07	71.2	16.1	12.2	14.5	85.6	16.6	70.7	15.8	1	27.1	55.4	23.2
2011	9	389.61	11	15.8	4.4	10.8	93.1	11.9	43.4	11.1	1.4	22.1	1.7	18
2011	10	392.45	1.8	10.1	0	2.4	21.1	6.7	999999	5.8	0	15.6	36.9	9.9
2011	11	393.00	4.2	3.3	0	-2.6	11.5	0.9	0.7	-0.3	0	6.7	12.7	0.2
2011	12	394.78	0	1.8	0	-6.6	1.1	-7.1	0.2	-7.5	3.5	-3.3	12.1	-9.1
2012	1	397.90	0	-1.1	1.8	-12.5	3	-10.3	4.4	-9.8	2.4	-7	9.2	-15
2012	2	398.72	0	3.8	0.4	-8.7	2.2	-6.3	5.1	-5.6	3.1	-0.2	18.4	-12

Citation: Liu Y, He Y, Wang Y, Gao Z (2023) Rapid Stabilization on Global Atmospheric CO_2 Concentrations by Cheaply Enhanced Tibetan Geological Carbon Sink. Int J Earth Sci Geophys 9:064

2012	3	398.15	0.7	6.6	0.8	-4.5	8.1	1	11.9	0.3	11.1	8.9	25.6	0.5
2012	4	398.33	999999	8.9	1.4	1.3	6.9	8.4	40.3	6.6	0	18.5	5.9	14
2012	5	397.70	21.5	15.1	0.2	5.1	76.4	12.4	49.4	11.2	5.5	21.3	25.9	18.7
2012	6	393.19	999999	18.1	0.2	10.9	58.6	15.4	999999	14.8	33.4	24.3	24.9	23.7
2012	7	387.88	132.5	16.9	0.3	16.3	147.7	17.2	101.4	16.1	3.5	26.1	27.6	24.6
2012	8	387.64	999999	16.7	999999	14.4	61.8	16.4	999999	16.2	15.7	26.1	10.1	23.7
2012	9	391.55	24.8	15.2	999999	10.7	57.4	11.9	18.5	11.8	0	22.3	34.2	18.1
2012	10	394.79	1.5	9.9	0	-0.2	20.2	5.8	10	5.1	0	14.1	32.3	8.9
2012	11	396.34	0	3.8	0	-5.2	3.1	-2.8	2.6	-2.7	0	5	44.2	-3.9
2012	12	397.61	0		0		0.7	-6.5	0.1	-6.2	3.1	-1.1	28.6	-12.6
2013	1	397.44	0	-0.3	3.6	-16.1	0	-8.7	0	-8.4	0	-3.4	7.1	-10.3
2013	2	397.39	0	2.9	7.6	-16.2	1.3	-3.2	4.8	-1.9	0	3.4	11.7	-10.1
2013	3	399.63	1.5	6.3	0.1	-5.5	0.9	4.4	0	3.8	0	14	13.2	5.5
2013	4	403.05	17.2	9.1	0	0.7	18.6	8.9	10	8	0	19	69.2	12.4
2013	5	402.74	50	13.1	0	5.7	67.6	12.3	30	11.2	22.4	20.9	27.1	16.6
2013	6	397.61	129.8	17.1	40.3	12.9	68.1	16.3	54.2	16.9	9.9	25.8	31.3	21.5
2013	7	393.52	164.4	16.8	12.8	15.7	74.5	16.9	999999	16.8	11.5	26.7	23.3	23.6
2013	8	392.26	80	15.9	37.4	14.6	107.9	18.2	40.1	18.8	0.3	26.9	29.2	22.8
2013	9	393.31	62.1	13.6	8.3	9.5	54.9	11.4	43.4	11.1	0.3	22.2	12.7	17.5
2013	10	395.83	38.4	8.7	0.9	3.7	10.5	6.7	15.6	5.9	0	16.4	16.6	11.4
2013	11	397.37	0.7	3.8	0	-5.1	6.7	-2	2.7	-2.5	0	4.2	44.5	0.2
2013	12	398.78	0	0	0	-8.5	2.6	-8.3	4.1	-8.2	0.1	-1.4	15	-6.8
2014	1	399.00	1.2	0	1.4	-12	0	-7.5	0	-7.4	0	-1.8	8.2	-10.9
2014	2	401.34	0	3.7	7.8	-11.2	1	-4	2	-3.5	0.4	1.8	20.6	-13.7
2014	3	404.93	5.7	5.8	0.5	-5.2	1.9	2.9	1.5	2.6	0	10.7	26.4	-0.2
2014	4	404.22	6.5	9.1	0.9	0	48	7.9	38.2	7.2	0.2	17.5	68.1	10.4
2014	5	402.14	9.5	14.5	0	5.3	26.1	11.7	9.7	11.1	0	21.5	32.5	17.7
2014	6	398.39	55.8	18.3	2.7	10.6	109.3	15.4	71.1	14	24.1	24.1	6.1	22.1
2014	7	393.32	258.9	16.4	32	14.7	86.4	17.1	74.2	16.6	10	26.9	21.3	24.3
2014	8	391.81	213.8	15.4	0.6	14.5	59.3	14.8	73.6	14.1	0	25.1	6.1	23.4

Citation: Liu Y, He Y, Wang Y, Gao Z (2023) Rapid Stabilization on Global Atmospheric CO_2 Concentrations by Cheaply Enhanced Tibetan Geological Carbon Sink. Int J Earth Sci Geophys 9:064

2014	9	394.93	999999	14.1	0	10.5	71.6	12.6	54.1	11.7	0	21.6	29.9	16.9
2014	10	398.15	2.3	8.9	2.3	2.3	32.2	7	25.4	6.1	0	15.3	24	9.3
2014	11	399.33	2.3	4.9	0	-3.7	9.4	-1.4	1.8	-1.4	0	5.3	31.6	-0.1
2014	12	400.00	0	1.7	0	-8	0	-7.9	0	-7.1	0	-3.5	22.2	-10.8
2015	1	401.83	5.5	-1	1.6	-11.3	1.1	-6.3	1.6	-6.8	0.8	-1	15	-8.7
2015	2	403.57	18.9	0.9	2	-8.3	0.6	-3.1	1.8	-3	0.8	3.6	15	-6.6
2015	3	404.31	0.1	7.3	5.5	-5.5	3.8	3.1	0.6	3.2	0	12.3	14.5	1.6
2015	4	405.28	8.7	9.2	0	1.2	15.4	8.6	37.8	6.9	0	18.3	55	12
2015	5	403.60	9.6	13.5	0.4	6	21.7	12.4	38.7	11.3	9.6	22.8	23.7	19.1
2015	6	399.04	60.5	18	13.8	10.1	51.8	15.9	79.2	14.7	10.5	24.1	74.3	21.7
2015	7	396.03	63.8	17.6	55.4	14.3	71.9	16.5	56.6	15.8	1.3	29.6	3.8	26.6
2015	8	394.81	134.8	15.9	59.5	14	61.1	15.5	53.4	14.8	2.7	25.9	53.9	23
2015	9	397.89	37.3	16.1	0	9.4	45.7	12.3	29.9	11.6	9	20.5	36.5	14.5
2015	10	401.47	0.5	10	0	2.6	25.9	7	6.3	6.4	0	15.5	33.4	8.8
2015	11	402.57	0	4.9	0	-2.6	5.9	1.1	2.2	0.7	0	7.1	32.7	0
2015	12	404.06	0.3	1.2	0	-8.1	1.3	-6.3	0.8	-7.5	1.8	-1.2	51.1	-6.6
2016	1	405.41	0	999999	0	999999	0.4	-8.5	1.1	-8.5	0.2	-1.8	12.6	-11
2016	2	405.85	0	5.98	0	-6.3	2.5	-5	0.9	-4.8	1.4	2.38	6.2	-9.38
2016	3	407.97	0.4	6.88	0	-1.78	28.1	2.9	18	2.8	0	12.93	14.2	2.8
2016	4	409.90	2	10.88	0	2.7	16.4	9.28	16.3	7.9	0	19.7	48.5	13.5
2016	5	407.87	74.2	12.7	0.4	8.2	60	11.8	59.2	10.9	2.1	22.3	46	15.88
2016	6	402.14	144.7	15.4	3.8	13.9	41.7	16.5	72.5	14.8	2.9	27.6	70.5	23.6
2016	7	398.67	166.2	16.3	32.6	15.7	84.8	18.6	141	17.3	1.7	27.9	40.6	24.4
2016	8	401.05	16.3	16.6	22.2	14.9	67.8	20.1	84.4	18.7	20.3	22.5	24.4	23.3
2016	9	403.01	44.1	13.7	0.3	11.1	81	12	53.4	10.7	21	21.5	0	20.9
2016	10	404.80	0	11.1	0	3.2	61.8	6.7	17.4	6.2	0	14.3	64	5.3
2016	11	406.95	0	4.5	0	-3.2	0.4	-0.2	0	-0.6	0	6.5	43.6	-3.2
2016	12	407.45	0	1.8	0	-5.1	1.6	-4.7	0	-5	0	1.1	15.9	-5.1
2017	1	408.33	0	0.11	0	-9.6	0	-6.7	0	-7.23	3	-3.54	4.7	-11.27
2017	2	409.78	0	4.5	0.4	-6.3	2.4	-2.3	4.2	-2.5	10.8	3.1	32.4	-8

Citation: Liu Y, He Y, Wang Y, Gao Z (2023) Rapid Stabilization on Global Atmospheric CO_2 Concentrations by Cheaply Enhanced Tibetan Geological Carbon Sink. Int J Earth Sci Geophys 9:064

2017	3	410.50	2.6	5.9	2.8	-3.9	9.9	1.1	7.5	0.4	2.7	10.4	6.6	-2.8
2017	4	411.95	2.9	10.02	5.8	2.26	29	7.61	12.5	6.9	22.1	17.21	54.2	11.07
2017	5	411.78	16.8	13.37	16.4	6	75.6	11.82	49.9	10.19	8.6	23.59	38.6	18.65
2017	6	407.47	176.9	16.1	6.8	10.9	40.6	15.3	55.1	13.6	6.3	25.6	40.7	23.1
2017	7	402.54	152.3	16.5	68.8	15	50.1	20.2	83.7	18.6	14.7	25.3	3.8	26.7
2017	8	401.55	164.3	16.38	27.5	14.7	121.2	16.6	73	15.4	11.7	24	22	22.2
2017	9	403.35	27.7	16.2	2.1	10.3	90.5	12.4	51	11.5	0	22.2	8	17.1
2017	10	405.50	8.7	11.6	0	3.2	33	6.7	14.2	5.7	1.8	14.3	20	7.5
2017	11	408.16	0	4.5	0	-4	0	-0.7	0.2	-1.7	0	6.9	40	1.6
2017	12	409.81	0	2	1.5	-6.9	0.8	-6.4	2.2	-6.5	2	-1	29.8	-6.9
2018	1	410.56	0	1.3	0	-7.6	2.3	-7.7	1.3	-7.5	0	-3.2	9.4	-16.4
2018	2	411.11	1.4	4.5	0.8	-6.2	0.1	-5.8	0.5	-5.1	0	1.4	3.9	-9
2018	3	411.99	8.4	5.5	0.4	-2.8	2.1	4.9	5.1	3.2	0	14.6	23.7	7.1
2018	4	414.52	7.6	9.1	0	2.8	30.2	8.5	28.3	7.2	1.4	18.03	52	11.6
2018	5	411.89	36.2	13.2	0.3	5.88	37.5	13.6	61.6	11.7	16.5	21.1	53.9	15.8
2018	6	405.59	70.8	17.3	3.1	13.4	55.8	17.1	54.7	14.6	3	24.5	6.9	23.1
2018	7	404.79	189.9	16.4	36.7	15.2	113	18.3	121.6	17.1	14.3	27.1	13.8	24.9
2018	8	406.44	175	16.2	39.7	15	136.6	17.7	142.1	16.3	14.3	25.3	41.3	23.9
2018	9	406.63	33.7	15.4	11.2	9.88	80.5	12.3	61.5	11	0	21.1	39.5	15.4
2018	10	409.16	0.2	9.1	0	-0.2	31.4	5.7	24.7	3.3	0	13.6	45.4	8.9
2018	11	410.18	0	4.7	1.1	-4.1	28.8	-1.8	20.9	-2.4	17.2	5	23.1	-3.6
2018	12	410.63	12	-1.7	0	-9.5	0.6	-7	1.4	-6.6	0	-3.3	22.2	-12.4
2019	1	412.10	0	-1.9	2.9	-12.6	2.4	-7.2	3.3	-8.3	7.6	-3.7	2.5	-11.3
2019	2	412.61	0	3.1	2	-9.4	2.4	-3.1	1.6	-3	0.3	2	11.5	-11
2019	3	413.17	3	5.8	0	-5.28	4.1	2.65	4	0.5	0	11.7	0	1.1
2019	4	415.34	6.7	9.7	0	3	22	10.3	11.4	8.7	0	20.8	23.5	13.4
2019	5	415.06	29	14.3	0.6	5.1	52.4	11.4	54.5	10.3	0	21.2	61	14.9
2019	6	408.72	2.7	19.6	0	9.9	95.8	14.7	86.7	13.9	36.1	23	15.6	21.9
2019	7	404.02	202.3	16.3	63	999999	69.8	16.5	75.3	15.3	1.4	28.1	6.7	25.7
2019	8	405.16	133.2	16.8	44.9	13.85	129.3	16.6	53.3	16	0.2	26.1	5.4	24.9

Citation: Liu Y, He Y, Wang Y, Gao Z (2023) Rapid Stabilization on Global Atmospheric CO_2 Concentrations by Cheaply Enhanced Tibetan Geological Carbon Sink. Int J Earth Sci Geophys 9:064

ISSN: 2631-5033

2019	9	408.76	101.1	14.4	4.5	999999	125.3	12.3	85.3	11.4	17.3	21.3	31.7	19.1
2019	10	412.16	11.5	10.3	0	2.5	29.4	6.6	39.5	5.5	0	14.9	13.9	9.9
2019	11	413.94	1.5	6.1	0.7	-2.8	2.5	0.9	2.7	-0.8	0	6.7	36.7	-1.9
2019	12	414.40	0	0.3	1.3	-11	1.1	-5.3	0.9	-8.4	0	-0.8	18.4	-7.6
2020	1	415.09	0.3	-0.7	3.6	-12.1	4.8	-5.3	2.1	-6.5	0.4	-1.8	9.7	-9.3
2020	2	415.71	0.2	1.7	0	-9.4	1.6	-2.4	0.4	-4.3	0	4.4	6.3	-4.8
2020	3	417.07	10.2	5.9	2.6	-4.2	5.1	2.8	7.9	1.7	0	11.8	18.6	2.9
2020	4	418.80	9.1	7.8	2.2	1.4	3.9	6.6	16.2	5.3	17	17.6	1.3	16.4
2020	5	418.25	36	11.9	2.4	6.3	62.9	11.7	47.1	10	15.1	22	19.6	19.9
2020	6	412.86	76.9	999999	6.3	999999	64.1	999999	71.8	999999	13	999999	38.2	21.8
2020	7	406.69	174.2	17.2	5.4	15	87	16.8	89.5	15.9	2.2	26.3	24.1	23.8
2020	8	406.87	79.1	17.18	0.3	16.8	123.6	16.1	95.5	15.4	0.4	26.6	29.9	23.3
2020	9	413.05	40.8	16.8	0	11.18	72.7	12.4	31.7	12.4	0	21.7	5.1	16.1
2020	10	416.45	1.3	13.1	0	2.9	2.4	6.2	7.4	5.1	0	13.2	23.1	8
2020	11	416.50	0	5	0.2	-4.9	3.1	0.7	0	-0.5	1.1	4.6	15.9	-1.3
2020	12	416.07	0	2.8	0	999999	1.6	-7.1	0	-7	0	-2.8	8.8	-12.3

All data are from the meteorological stations of China Meteorological Administration labelled in Figure 1. 999999 means data-free. P: Precipitation; T: Temperature; CO_2: Atmospheric CO_2 concentrations.

Citation: Liu Y, He Y, Wang Y, Gao Z (2023) Rapid Stabilization on Global Atmospheric CO_2 Concentrations by Cheaply Enhanced Tibetan Geological Carbon Sink. Int J Earth Sci Geophys 9:064

high topography corresponds to thickened crust, and vice versa. Therefore, the formative ages of the oldest thickened crust are generally regarded as the originally uplifting times of the proto plateau [20]. Previous studies have revealed that the oldest Tibetan thickened crust as a result of the continuous India-Asia collision [21] had been formed during the Eocene-Oligocene transition [20,22-23], corresponding to the formation of the Antarctic ice sheets exactly [16-17]. It has thus confirmed the previous view that the uplift of Tibetan plateau led to the global cooling and subsequent formation of the Antarctic ice sheets, largely due to intensive silicate chemical weathering [24-27]. Recent studies have further revealed that approximately 7 trillion tonnes of atmospheric CO_2 have been transformed to organic matters, carbonates and particularly carbonic magmas [28], lately trapped in the Tibetan thickened crust and its adjacent foreland basins since the Eocene-Oligocene transition by the uniquely flat subduction of Indian continent below Tibetan plateau [29-31], leading to the formation of glacial-interglacial climate [24-27]. The long-term imbalance between atmospheric inputs and outputs of CO_2 [14-17] could be perfectly accounted for by the fact that huge amounts of atmospheric CO_2 had been persistently accommodated by the growing Tibetan plateau [29-31], the only nascent carbon reservoir worldwide [30,31]. The formation of Tibetan plateau is thus an important global rather than regional event, driving the global climate change, as well as the fluctuation of global atmospheric CO_2 concentrations since the Eocene-Oligocene transition [30,31]. However, most Tibetan regions are barren deserts now (Figure 1) that are carbon sources rather than carbon sinks [31]. It is therefore a critical issue whether currently large anthropogenic emissions can be sequestered by the Tibetan geological processes within one year rather than one million years. Within a short-term time, traditional silicate chemical weathering plays a tiny role in the direct removal of atmospheric CO_2 outside of the unique Tibetan plateau, largely due to extremely low chemical reaction rates [32], so that the traditionally geological carbon sink is generally neglected [9]. However, the global carbon budgets have clearly shown that the land carbon sink is stably increased greatly [6,9-10]. It is still unknown where regions and what mechanisms are primarily responsible for the persistently enhanced land carbon sink [6,9-10], unfortunately. In addition, many studies have indicated that inland waters play an important role in the global carbon cycle [33]. Numerously inland salty lakes and/or wetlands occurs in Tibetan plateau and its northern neighboring regions (Figure 1). It is also unclear what contributions these inland salty lakes or wetlands make in the global carbon sink. These questions critical to the public worldwide are well addressed in this study. And it has been clearly illustrated how fast and cheaply the large amounts of anthropogenic emissions are transformed to massively renascent carbonates and relatively minor organic carbon matters that are later buried in the Tibetan thickened crust and its adjacent foreland basins by the uniquely Tibetan geological processes. Subsequently the cheapest approach is present here to rapidly stabilize global atmospheric CO_2 concentrations regardless of how much anthropogenic emissions in the near future.

Materials and Methods

Data acquisition and analysis

The entire Tibetan plateau and its adjacent regions including the Urumqi area in the northwest are research regions in this study (Figure 1). In order to quantitatively evaluate carbon uptake capacity of the critical regions (Figure 1) in the context of massive anthropogenic emissions today, abundantly observational multidisciplinary data were collected for comprehensively contrastive analyses (Table 1, Table 2, Figure 1 and Figure 2). Horizontal shortening rates between Indian and Asian continents (Figure 1) were from [34], indicating the deformative intensity of crust triggered off by the consecutive collision between Indian and Asian continents. From the Lhasa and Shiquan River regions in the south to the Urumqi and Xining regions in the north roughly, the crustal deformation is gradually decreasing [34] (Figure 1). Numerous observational data of precipitation and temperature were collected from the meteorological stations except Waliguan station within the studying regions (Table 1 and Figure 1). The Waliguan station recording atmospheric CO_2 concentrations professionally is situated on the top of Mt. Waliguan on the NE Tibetan plateau (Figure 1). The predominant wind directions of this station are from SW to NW (summer) and from ESE to NE (winter). The air sample collection and subsequent measurements of atmospheric CO_2 concentrations were reported in previous studies [35,36] in

Table 2: Annually mean precipitation and variations of atmospheric CO_2 concentrations over Tibetan plateau.

Year	Annual growth rate	Bimonthly growth rate	Annual C uptake rate	Lhasa	Shiquanhe	Xining	Qabqa	Hotan
1991	-1.48	2.64	5.12	476.3	33.6	243.2	278	39.3
1992	4.90	3.07	5.07	291.7	47.7	425.2	350.3	61.7
1993	-0.29	1.84	3.77	537.2	56.1	420.9	397.5	69
1994	2.95	2.45	5.65	371.8	73.3	418.1	290	62.9
1997	No data	2.22	3.87	321.5	53	409.9	312.9	10.6
1998	1.19	2.46	1.53	580.9	55.4	460.3	299.7	32.6
1999	2.60	1.98	3.69	538.1	116.4	411.9	308.6	32.3
2000	3.04	2.33	3.14	529.7	120.8	343	244	19.2
2001	-2.16	3.09	4.01	492.3	52.9	397.8	336.2	26
2002	2.84	2.18	2.36	539.3	104.8	387.7	316.8	63.8
2003	6.09	2.11	1.23	549.7	40.6	537.9	266.7	86.1
2004	2.23	3.69	3.37	555.2	35.6	429.5	359.3	40.3
2005	-0.79	0.46	3.81	490.3	42.7	484.1	377	88.4
2006	4.24	3.62	3.49	339.3	101.3	352.3	332.1	41.7
2007	-0.05	3.37	3.32	477.3	33.4	523.1	332.9	23.8
2008	3.58	2.82	4.29	533.8	80	378.6	353.6	34.3
2009	0.61	4.41	4.51	344	25.3	459.1	340.1	19.2
2010	3.95	2.32	3.29	359.8	91.1	405	328.8	111.9
2011	0.02	3.27	2.5	425.4	58	390.4	314.5	11.4
2012	1.72	-0.39	0.72	365.2	47.9	446.1	332.4	77.8
2013	4.62	5.66	4.27	565.2	111	413.6	275.7	44.5
2014	-0.45	3.59	4.93	637.8	48.2	446.5	351.6	34.7
2015	3.00	1.71	1.22	340	138.2	306.2	308.9	36.5
2016	3.86	4.05	2.45	551.6	59.3	446.5	464.2	49.6
2017	2.88	2.17	2.14	552.2	132.1	453.1	353.5	83.7
2018	3.24	3.41	3.89	535.2	93.3	518.9	523.7	66.7
2019	-0.77	2.73	0.94	491	119.9	536.5	418.5	62.9
2020	2.67	3.09	2.73	428.1	23	432.8	369.6	49.2

Annually mean precipitation data are recorded by the Tibetan meteorological stations labelled in Figure 1.

detail. Monthly mean data of atmospheric CO_2 concentrations in ppmv, rainfall in millimeters and temperature in degrees Celsius were listed in Table 1, respectively. Yearly mean rainfall data in millimeters were listed in Table 2. Additionally, in combination with the multidisciplinary data, comprehensive geological surveys have been performed to try to figure out the Tibetan carbon uptake mechanisms today.

Annual carbon uptake rates (in ppmv) were gotten by that the highest value in a year, the spring's value normally, subtracted the December's value. Bimonthly growth rates of atmospheric CO_2 concentrations (in ppmv) were acquired by that the year's highest value subtracted the February's data (Figure 2b). Annual growth rates (in ppmv) were acquired by the lowest value in a year, normally the summer's value, deducted the lowest one in the previous year (bottom to bottom) (Figure 2c). All of them were listed in the Table 2. Regional precipitations are sum of precipitation intensity of individual observatory stations (in millimeters) multiplied by precipitation areas (Figure 2b). Assuming all precipitation areas in each time in

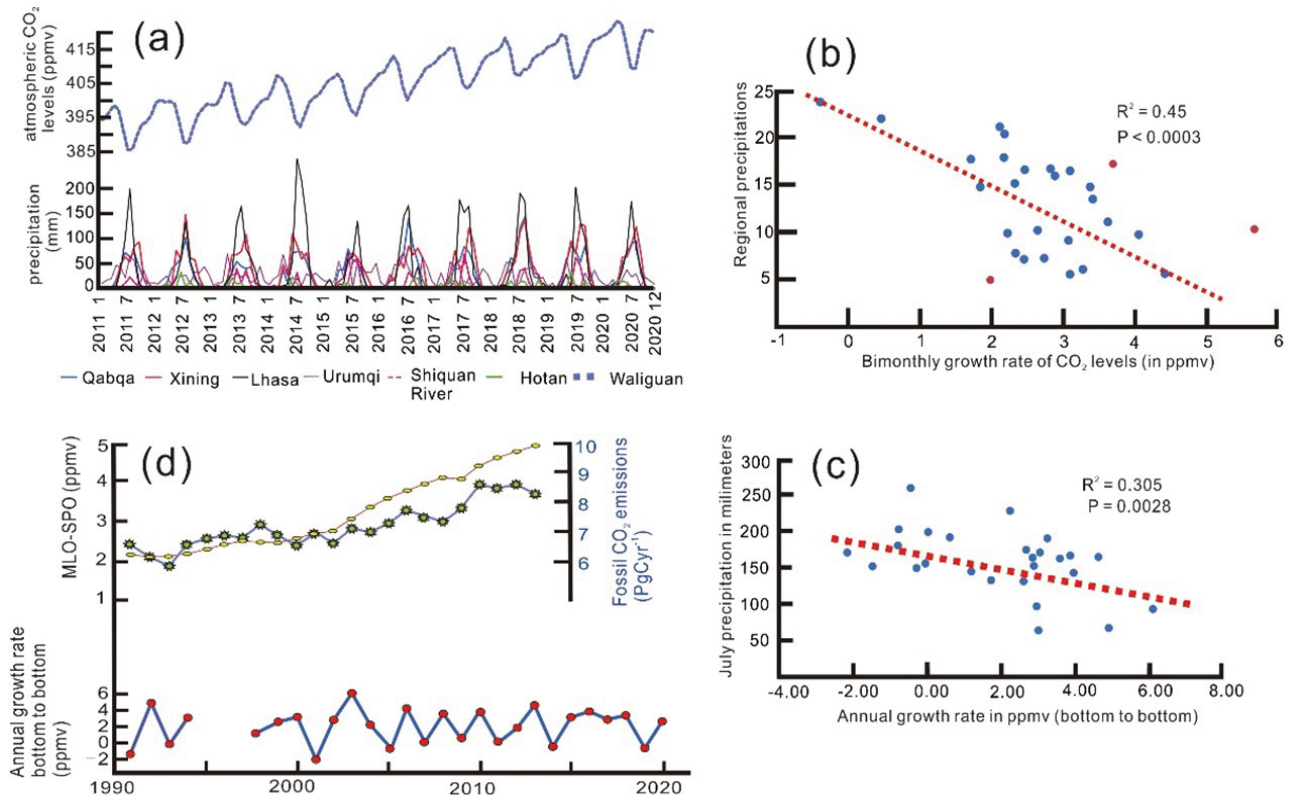

Figure 2: (a) Monthly mean records of atmospheric CO_2 and precipitation from 2011 to 2020. (b) Trend of regional precipitations and the bimonthly growth rates of CO_2 concentrations over the past 30 years. (c) Trend of July's precipitation in the Lhasa area and the annual growth rates of atmospheric CO_2 concentrations (bottom to bottom) over the past 30 years. (d) Comprehensive comparison between the annual growth rates of atmospheric CO_2 concentrations within Tibetan plateau (red circles in the lower part) and the interhemispheric CO_2 gradients (green polygons in the upper part), as well as CO_2 emissions from fossil fuel and cement (yellow ellipses in the upper part) [10].

each observatory station were as same as one unit. This led to large uncertainties in estimations of the regional precipitations in three red spots in the Figure 2b. These large uncertainties will be greatly diminished by extra numerous precipitation data from newly-added meteorological stations within Tibetan plateau in the near future. The EXCEL software was used to make regression analyses between the regional precipitations and the bimonthly growth rates during spring (Figure 2b), as well as the July's precipitation recorded by the Lhasa station (Figure 1 and Table 1) and the annual growth rates (bottom to bottom) (Figure 2c), respectively.

In order to deeply reveal the relations between the variations of atmospheric CO_2 concentrations recorded by the Waliguan station, Tibetan plateau (Figure 1) and the changes of global atmospheric CO_2 levels, the annual growth rates (bottom to bottom) were projected into the evolution of interhemispheric CO_2 gradient and of CO_2 emissions from fossil fuel and cement [10] for a comprehensive comparison (Figure 2d).

Tibetan carbon sink estimations

Two completely different methods were used to evaluate the carbon uptake by Tibetan plateau in this study. The first approach is from [31]. The primary reason for this method is that large amounts of atmospheric CO_2 had been rapidly turned into massively secondary carbonates and organic carbon that are subsequently buried in the thickened crust and its adjacent foreland basins by the uniquely geological processes [29-31]. The carbon uptake can be therefore acquired by the direct measurements on the contents of the secondary carbonates and organic carbon in soils and rocks beneath the soils within Tibetan plateau and its adjacent foreland basins [31]. The calculated formula for this estimation is following:

$$F = \rho^{*}S^{*}f^{*}(C_{org} + C_{inorg}) + Q \quad (1)$$

Where:

F = annual total atmospheric CO_2 uptake (in tonne);

ρ = average density (in tonnes per cubic meter);

S = average annual carbon burial rate (in millimeter per year), normally 1-2 millimeters per year due to horizontal shortening rates of 2 centimeters per year [34];

f = area of regions (in hectare);

C_{org} = buried organic carbon contents (in weight percent);

C_{inorg} = buried inorganic carbon contents (in weight percent);

Q = organic carbon over surface, roughly corresponding to the traditional ecosystem carbon sink (in tonnes per year).

The changing of CO_2 concentrations (in ppmv) was used as the second method that is relatively simple to estimate the carbon uptake by the entire Tibetan plateau and its adjacent regions in this study. The annual carbon uptake rates listed in the Table 2 roughly represent the net carbon uptake by these critical regions within one year. 1 ppmv = 7.782 gigatonnes atmospheric CO_2 [9].

Results and Discussion

Variability of atmospheric CO_2 concentrations within Tibetan plateau and its adjacent regions over the past 30 years

In general, within a year, the atmospheric CO_2 concentrations within Tibetan plateau rise during spring firstly, plummet largely during summer, and slightly decrease or roughly remain constant during winter (Figure 2a, Table 1 and Table 2). The large decline of atmospheric CO_2 levels is perfectly corresponding to July's heavy precipitation within the southern Tibetan plateau (Figure 2 and Table 1) where the horizontal shortening rates are the highest [34] (Figure 1). This region is therefore the most tectonically active silicate region due to the continuous collision between Indian and Asian continents (Figure 1). Whereas precipitation recorded by the Urumqi meteorological station, situated in the northern region outside of Tibetan plateau where the horizontal shortening rates are close to zero [34] and thus it is relatively tectonic stable (Figure 1), has little effect on the variations of atmospheric CO_2 concentrations (Figure 2a and Table 1). The regression analysis has further suggested that during spring, the bimonthly growth rates of atmospheric CO_2 concentrations are negatively correlated with Tibetan precipitations over the past 30 years (Figure 2b). For example, in the spring of 2012, the bimonthly growth rate was surprisingly as low as minus 0.39 ppmv (Table 2), largely due to heavy precipitation during this spring (Figure 2, Table 1 and Table 2). Moreover, the annual growth rates (bottom to bottom) were highly negatively correlated with the July's precipitation within southern Tibetan plateau where the tectonics are the most active (Figure 1, Figure 2, Table 1 and Table 2). For instance, in 2014, although the bimonthly growth rate was up to 3.59 ppmv (Table 2 and Figure 2) because of the cold, dry and windy weather during this spring (Table 1), the annual growth rate was incredible as low as minus 0.45 ppmv (Table 2 and Figure 2) and the annual carbon uptake rate was still up to 4.93 ppmv (Table 2), largely due to the July's heavy precipitation (Table 1). In 2015, although the bimonthly growth rate was as low as 1.71 ppmv due to relatively much water during this spring (Table 1, Table 2 and Figure 2), the annual growth rate was up to 3.00 ppmv, and the annual carbon uptake rate was only 1.2 ppmv, partially owing to the relatively less precipitation during July (Table 1, Table 2 and Figure 2). Furthermore, the annual growth rates were roughly corresponding to the changing of the interhemispheric CO_2 gradient [10] (Figure 2d). For example, in 2003, the annual growth rate was up to 6.09 ppmv (Table 2), roughly corresponding to the peak of the interhemispheric CO_2 gradient (Figure 2d). This suggested that the annual growth rates of atmospheric CO_2 concentrations in Tibetan plateau (Table 2) probably represented the evolution of global atmospheric CO_2 concentrations. That further implies that if we control the rise in the Tibetan atmospheric CO_2 concentrations in the near future, we could restrain the increasing in global atmospheric CO_2 concentrations quickly.

During spring, most of Tibetan plateau and its adjacently northern regions were cold and dry (Table 1) and strongly windy, resulting in strong physical weathering, as well as relatively weak silicate chemical weathering and photosynthesis owing to water shortage and relatively low temperature in spring (Table 1). Tibetan previously-

formed organic-carbon-bearing soils disappeared partially (Figure 3), becoming sources of sand storms. Oxidization of soil organic carbon releases large amounts of CO_2 into atmosphere once again, leading to the formation of a carbon source in the case of water shortage particularly during spring (Table 1, Figure 2 and Figure 3). The bimonthly growth rates of atmospheric CO_2 concentrations

Figure 3: Field photo showing that Tibetan previously organic-carbon-bearing soils (yellow brown) disappeared partially, and subsequently light-colored cracked granites below the soils were exposed in the air to experience the traditional silicate chemical weathering, largely owing to stronger physical weathering.

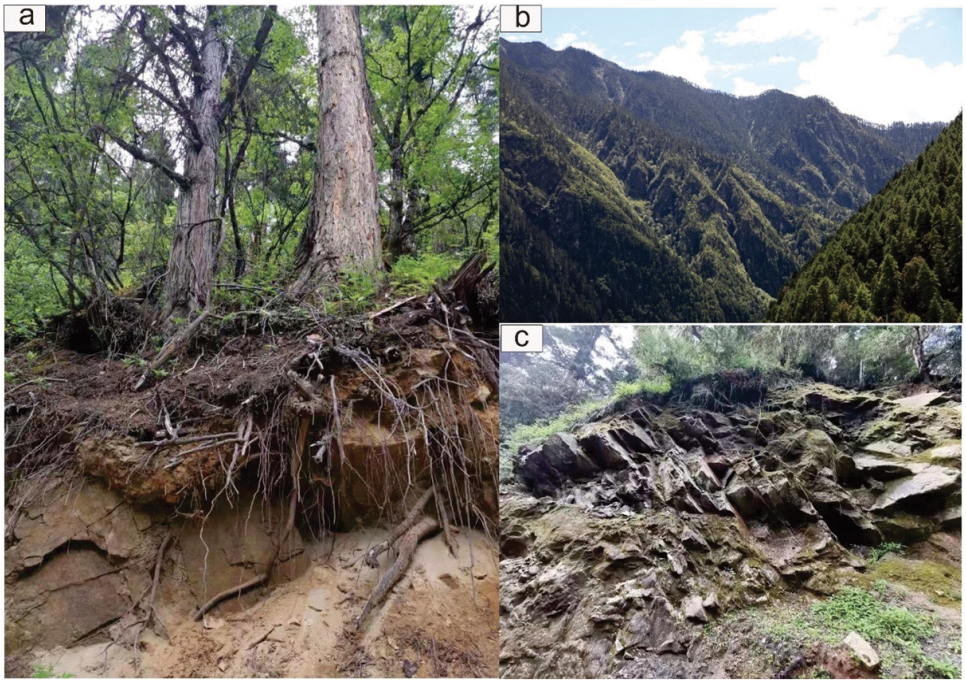

Figure 4: Field photos show that a large amount of freshwater and atmospheric CO_2 is continuously sent to the Tibetan deep silicate regions where the tectonics are the most active through coupled the active tectonics and young tree roots. (a) The subsurface cracked silicates underwent intensive carbonization entirely and thus became yellow brown, due to the actively young tree roots. (b) The entire mountain fully covered by trees was strongly deformed so that a large amount of freshwater and atmospheric CO_2 can be sent to the deeply cracked silicate regions along the large joints consecutively. (c) The strongly deformative granites were quickly turned into fine-grained yellow-brown secondary carbonates and clay minerals due to the active tectonics and young tree roots. Newly-formed organic matters were easily trapped by the secondary clay minerals.

(Table 2) are therefore controlled largely by the Tibetan surficial water.

Enhanced subsurface silicate chemical weathering

Intensive crust horizontal shortening triggered off by the India-Asian convergence in succession (Figure 1) resulted in the strongest deformation of the southern Tibetan silicates (e.g., Figure 3, Figure 4, Figure 5 and Figure 6). Abundant (micro) fractures therefore occurred in the southern Tibetan silicates normally (Figure 3, Figure 4, Figure 5 and Figure 6). Much freshwater is transferred to Tibetan plateau by heavy precipitation particularly during July (Table 1 and Figure 2a), leading to much surficial freshwater in locally cracked silicate regions (e.g., Figure 4 and Figure 5). Plants are thus actively growing up within the freshwater-enriched cracked silicate regions only during summer (e.g., Figure 4 and Figure 5). Through the most physiologically active plant roots within two months (Figure 4 and Figure 5), a large amount of freshwater and atmospheric CO_2 can be continuously sent to the Tibetan subsurface cracked silicate regions, subsequently transformed to high concentrations of organic and carbonic acids, respectively [37-40]. The local subsurface CO_2 concentrations can be up to 50,000 ppmv [38], as most of CO2released by the plant roots and soils are subsequently trapped by the planting wetlands and subsurface clay minerals (Figure 4 and Figure 5), much better covers against the escape of CO_2 from the Tibetan water-enriched soils.

Whereas in the water-shortage silicate regions where the tectonics are also the most active (e.g., Figure 3), the plants are still the least physiologically active even during summer (e.g., Figure 3), largely due to the less precipitation. Little atmospheric CO_2 and water are therefore sent to the subsurface cracked silicate regions (e.g., Figure 3). The light-colored cracked silicates exposed in the air (e.g., Figure 3) have to experience the traditionally silicate chemical weathering, but its carbon uptake can be ignored completely because of little formation of secondary carbonates nor organic matters (e.g., Figure 3). These fractured silicates could remain stable in the air for a long time in the case of water-shortage (Figure 3).

Within the 3D space beneath the Tibetan planting wetlands where the tectonics are the most active (e.g., Figure 4, Figure 5, Figure 6 and Figure 7) rather than the 2D space where the conventional silicate chemical weathering takes normally place (e.g., Figure 3), the subsurface cracked silicates can chemically react completely with the large amounts of organic and carbonic acids with high concentrations exuded by the extremely physiological active plant roots in succession during

Figure 5: Tibetan soil section showing that despite of at an altitude of 5100 meters, various grasses are growing well in the freshwater-enriched broken silicate regions during summer, leading to the enhancement of silicate chemical weathering beneath the dark soil. Massive secondary carbonates (yellow brown) below the dark soil and organic matters (dark) are therefore formed in succession at relatively high-altitude regions at the expense of huge amounts of atmospheric CO_2.

Figure 6: Rock cores showing that the deep cracked silicates underwent intensive carbonization. Large amounts of fine-grained yellow-brown secondary carbonates and clay minerals were therefore formed in the extremely deep silicate regions beneath the forest-wetlands. The secondary clay minerals held newly-formed organic matters normally.

summer (Table 1, Figure 4, Figure 5, Figure 6 and Figure 7). All weaknesses of the traditional silicate chemical weathering (e.g., Figure 3) are perfectly overcome, such as very short residence time of atmospheric CO_2 with very low concentrations for the silicate chemical weathering reactions (e.g., Figure 3), extremely small surface areas available for these chemical weathering reactions (e.g., Figure 3), conventionally higher pH values against the reactions, and relatively low temperature for the chemical reactions [32,40]. Consequently, within the most tectonically active silicate region rich in surficial freshwater triggered off by the heavy precipitation during summer (Figure 4, Figure 5, Figure 6 and Figure 7), the Tibetan subsurface silicate chemical weathering rates are at least 1 million times that for the traditional silicate chemical weathering (e.g., Figure 3) during summer [32]. Moreover, the newly-formed organic matters exuded by the extremely physiological active plant roots are normally trapped by the subsurface secondary clay minerals. These lead to a large decline of atmospheric CO_2 concentrations in a very short time, only 30 days, in the context of massive anthropogenic emissions (Table 1 and Figure 2). More importantly, the recent drillings in the tectonically active forest-wetlands have further revealed that the Tibetan subsurface silicates, up to 2,500 meters depth, are still subject to the intensive silicate chemical weathering (Figure 6). This clearly suggests that the huge amounts of the organic and carbonic acids with higher concentrations exuded by the most physiologically active Tibetan plant roots continuously are further transferred to much more depths to react chemically with the deeply cracked silicates completely (e.g., Figure 6) by groundwater along deep fractures or even large faults that are also results of the continuous India-Asia collision (Figure 7). Thus, the subsurface silicate chemical weathering is further enhanced greatly so that the Tibetan forest-wetlands (Figure 4) boast a bottomless appetite for the capturing of large amounts of atmospheric CO_2 (Figure 7). This is the primary reason why the annual growth rates of the Tibetan atmospheric CO_2 concentrations (bottom to bottom) are strongly negative correlated with the July's precipitations within the most tectonically active silicate region (Table 1, Table 2 and Figure 2). The unique Tibetan subsurface silicate chemical weathering thus plays an important role in the rapid transformation of the vastly anthropogenic emissions to massively secondary carbonates and organic matters trapped in the clay minerals normally.

Enhanced chemical sedimentation

During winter, Tibetan plateau becomes an icy plateau, largely owing to global warming

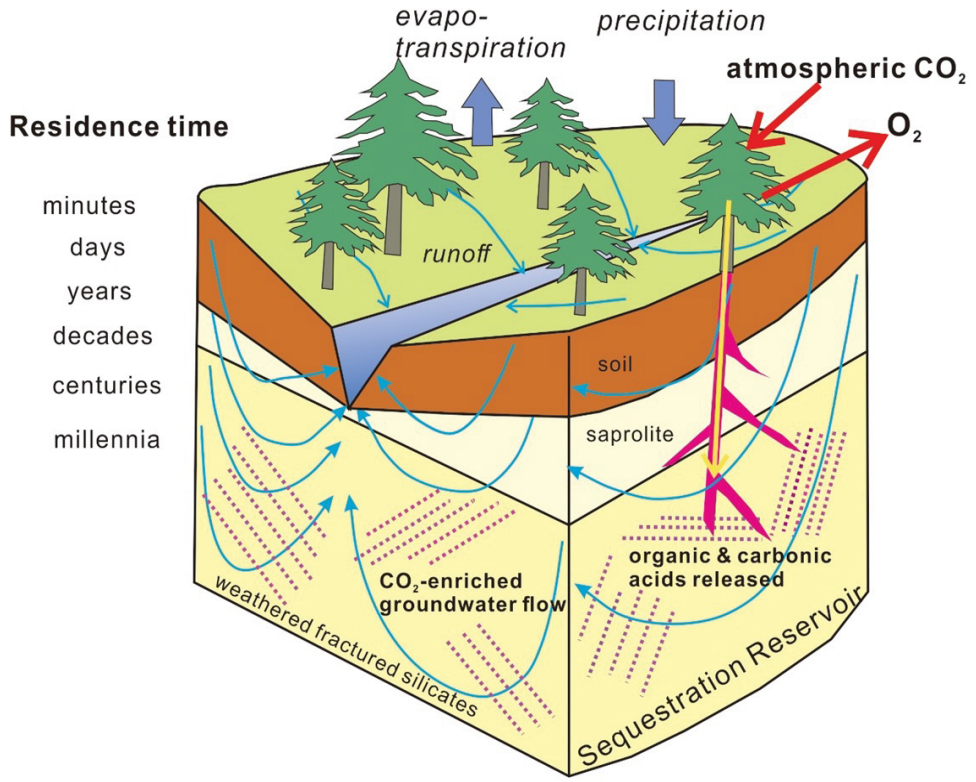

Figure 7: Schematic showing how huge amounts of freshwater and atmospheric CO_2 are sent to the deep regions in succession and subsequently transformed finally to massively secondary carbonates and organic matters surrounded by the secondary clay minerals normally beneath the tectonically active freshwater-enriched silicate regions. The residence times of meteoric water vary from minutes for surface runoff to millennia for deeply circulating groundwater, after [41].

Figure 8: Lacustrine carbonates (white layer) were formed in the salt lakes within northern Tibetan plateau during winter.

[31,32,42,43], so that sunlight actually goes back to outer space by the massive snow or ice sheets at an altitude of over 4000 meters. This leads to a weak greenhouse effect in Tibetan plateau despite of relatively high atmospheric CO_2 concentrations during winter, typical negative feedbacks between

the growing Tibetan plateau and global climate change during winter. Under relatively low temperature during winter (Table 1), particularly up to minus 40 degrees Celsius in the northern Tibetan plateau during night, large amounts of Tibetan plants rapidly die in the planting wetlands and massive carbonates fast crystallize from the numerously salty lakes in Tibetan plateau (Figure 1). Subsequently, massive carbonates and/or minor organic matters are quickly deposited in the bottom of the salty lakes (Figure 8) and/or planting wetlands (Figure 9), consuming extra large amounts of atmospheric CO_2 (Table 1 and Figure 2a). The inland waters within the central Asia including the salty lakes and planting wetlands (Figure 1) play an important role in the global carbon sink so that the Tibetan atmospheric CO_2 levels remain stable roughly or even decrease slightly in the context of much more anthropogenic emissions for heating during winter generally (Table 1 and Figure 2).

Tectonic burial

Tibetan plateau has been featured by the active tectonics triggered off the continuous collision between Indian and Asian continents (Figure 1, Figure 3, Figure 4, Figure 5 and Figure 6). The massively secondary carbonates and organic carbon (Figure 4, Figure 5, Figure 6, Figure 7, Figure 8 and Figure 9) transformed fast from the huge anthropogenic emissions are further trapped in the Tibetan thickened crust and its adjacent foreland basins [29-31] by the active tectonics (Figure 10 and Figure 11). And subsequently, some of them will experience intensive decarbonization in the deep regions beneath Tibetan plateau by the persistently flat subduction of Indian continent beneath Tibetan plateau, releasing the carbonic magmas to the specific magma chambers in the thickened crust [28,29], and thus, resulting in the only nascent carbon reservoir worldwide [29-31]. Furthermore, the relics decarbonized in the deep regions are exhumated to shallow depth as little-weathered cracked silicates, subsequently undergoing the intensive carbonization such as the enhanced subsurface silicate chemical weathering (e.g., Figure 4, Figure 5 and Figure 6) once again, also as results of the persistently flat subduction of Indian continent beneath Tibetan plateau [29-31]. The large amounts of atmospheric CO_2 are therefore transferred persistently into the thickened crust. It is the major mechanism for large carbon uptake by the growing Tibetan plateau, leading to that global atmospheric CO_2 concentrations are never over 300 ppmv since the late Pleistocene [13]. Whereas within the regions outside of Tibetan plateau, the unique carbonization and decarbonization take never place due to the lacking of the distinguished active tectonics triggered off by the India-Asia

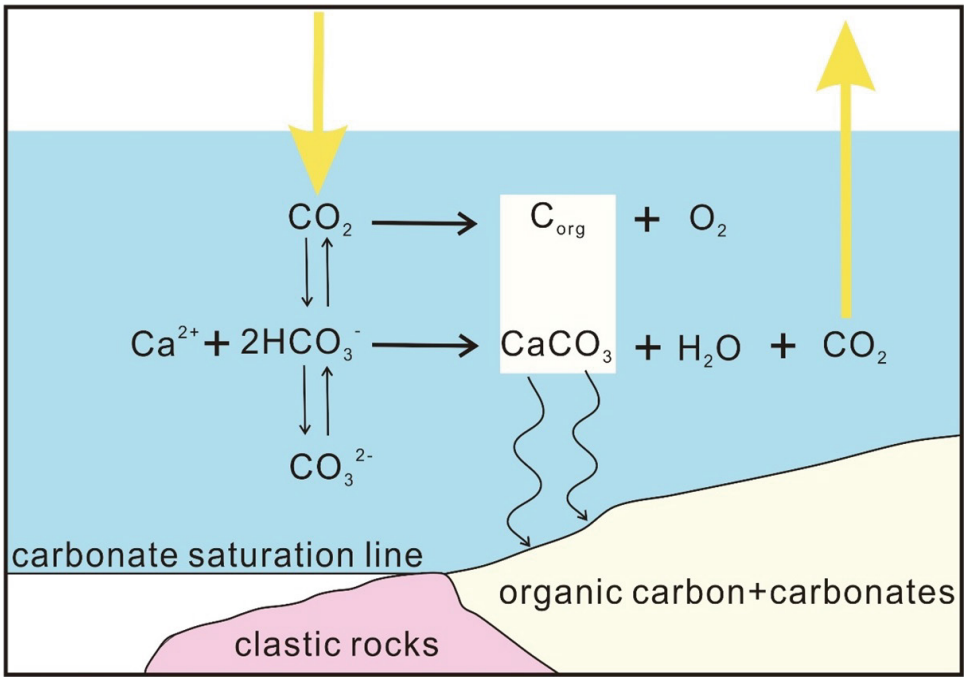

Figure 9: Schematic model showing massive carbonates and/or minor organic carbon are quickly deposited in Tibetan planting wetlands and salty lakes during winter.

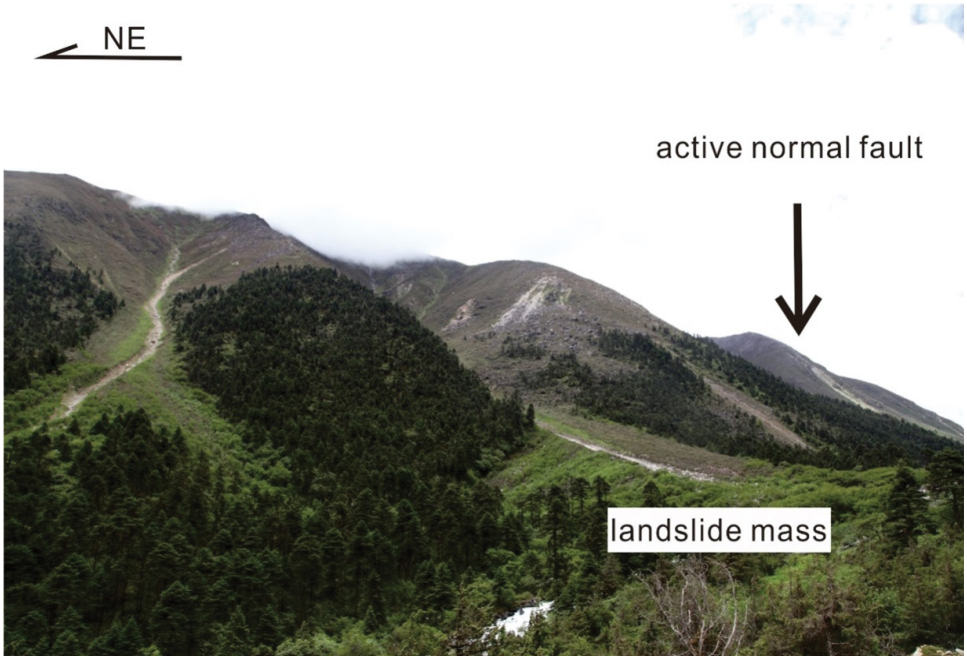

Figure 10: Field photo showing that landslides normally took place along the active normal fault, leading to the tectonic burial of massively newly-formed carbon-bearing materials within the tectonically active freshwater-enriched silicate regions.

Figure 11: Field photo showing tectonic burial of newly-formed organic matter and secondary carbonates due to the active tectonics.

collision in succession, and thus, large amounts of CO_2 are easily released into atmosphere once again. This is the primary reason why carbon sink saturation easily occurs in these regions outside of Tibetan plateau, such as African and Amazonian tropical forests [1,2], the Earth's largest tropical forests, and why the precipitation in the Urumqi area (Figure 1) has little impact on the variation of atmospheric CO_2 concentrations (Table 1, Table 2 and Figure 2a).

Implications

As mentioned above in detail, the carbon uptake rates of the well-known reservoirs have remained constant roughly or even decreased in recent decades [1-6], indicative of a positive carbon-

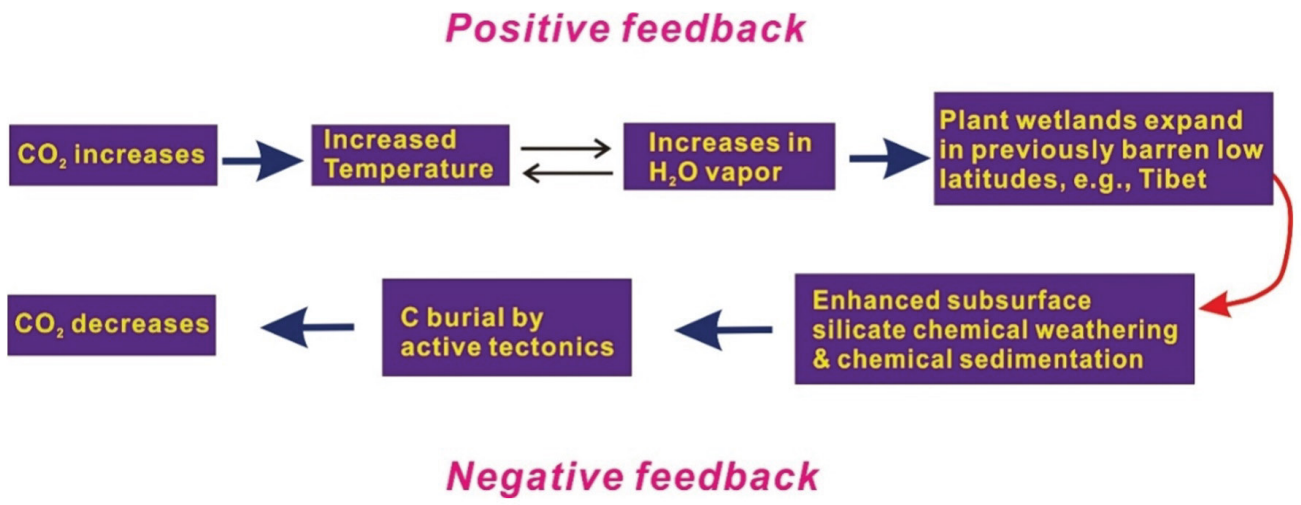

Figure 12: Schematic showing the negative feedback between the growing Tibetan plateau and global climate change to stabilize global atmospheric CO_2 concentrations quickly.

climate feedback [4]. However, the terrestrial carbon sink is stably increased [6,9,10]. Based on the global carbon mass balance, these reduced sinks must be more than compensated for by an increase in the rates of unfamiliar carbon uptake. The annual carbon uptake rates listed in the Table 2 have clearly shown that over the past 30 years, the Tibetan plateau and its adjacent regions are always a large net carbon sink even in the context of huge anthropogenic emissions, distinguished from other well-known carbon reservoirs [1-6]. Satellite remote investigations in combination with field surveys have further confirmed that Tibetan barren regions are rapidly transforming to the planting wetlands [30-31,43-45], due in large part to global warming [30,31,42], clearly suggesting higher inputs of organic carbon to Tibetan regions in succession [46-48]. More importantly, as demonstrated above in detail, the chemical sedimentation during winter and subsurface silicate chemical weathering during summer, as well as the tectonic burial are greatly enhanced along with the increasing of the Tibetan planting wetlands. Recent space-borne measurements of atmospheric CO_2 [49,50], the independent investigations approved by the IPCC, have further confirmed the surveys in this study that the currently eastern Tibetan plateau fully covered by various plants is a large carbon sink. Multidiscipline pieces of evidence have therefore revealed that the Tibetan plateau and its adjacent regions do be such regions where the net carbon uptake has been only increased greatly worldwide, resulting in strongly negative carbon-climate feedbacks (Figure 12 and Figure 13). Such negative feedbacks between the growing Tibetan plateau and global climate changes are the major mechanism (Figure 12 and Figure 13) to stabilize atmospheric CO_2 concentrations in the future. For example, Yarlung Zangbo, one of the largest rivers in Tibetan plateau, is a barrier lake now (Figure 14) due to the landslides triggered off by coupled the active tectonics and heavy precipitation. A large amount of freshwater and atmospheric CO_2 is consecutively sent to the deeply silicate region beneath the barrier lake to enhance the Tibetan geological carbon sink including the enhanced subsurface silicate chemical weathering during summer (e.g., Figure 7) and chemical sedimentation during winter (e.g., Figure 9), as well as the tectonic burial (e.g., Figure 10 and Figure 11). Therefore, the Tibetan geological carbon sink contributes greatly the recent increase in the terrestrial carbon sink that is roughly estimated to be 10 billion tonnes of atmospheric CO_2 per year [9]. This estimation is approximately consistent with the calculations of carbon sink based on the changing of atmospheric CO_2 concentrations recorded by the Waliguan station (Table 1 and Table 2). Over the past 30 years, most annual carbon uptake rates are more than 2 ppmv (Table 2), corresponding to uptake of more than 10 billion tonnes of atmospheric CO_2 per year [9] by the entire Tibetan plateau and its adjacent regions. Consequently, compared with the traditional ecosystem carbon sink, such as the carbon sink in the African and Amazonian tropical forests [1,2], the Tibetan geological carbon sink is an extremely large size that can easily affect the variations of the global atmospheric CO_2 levels

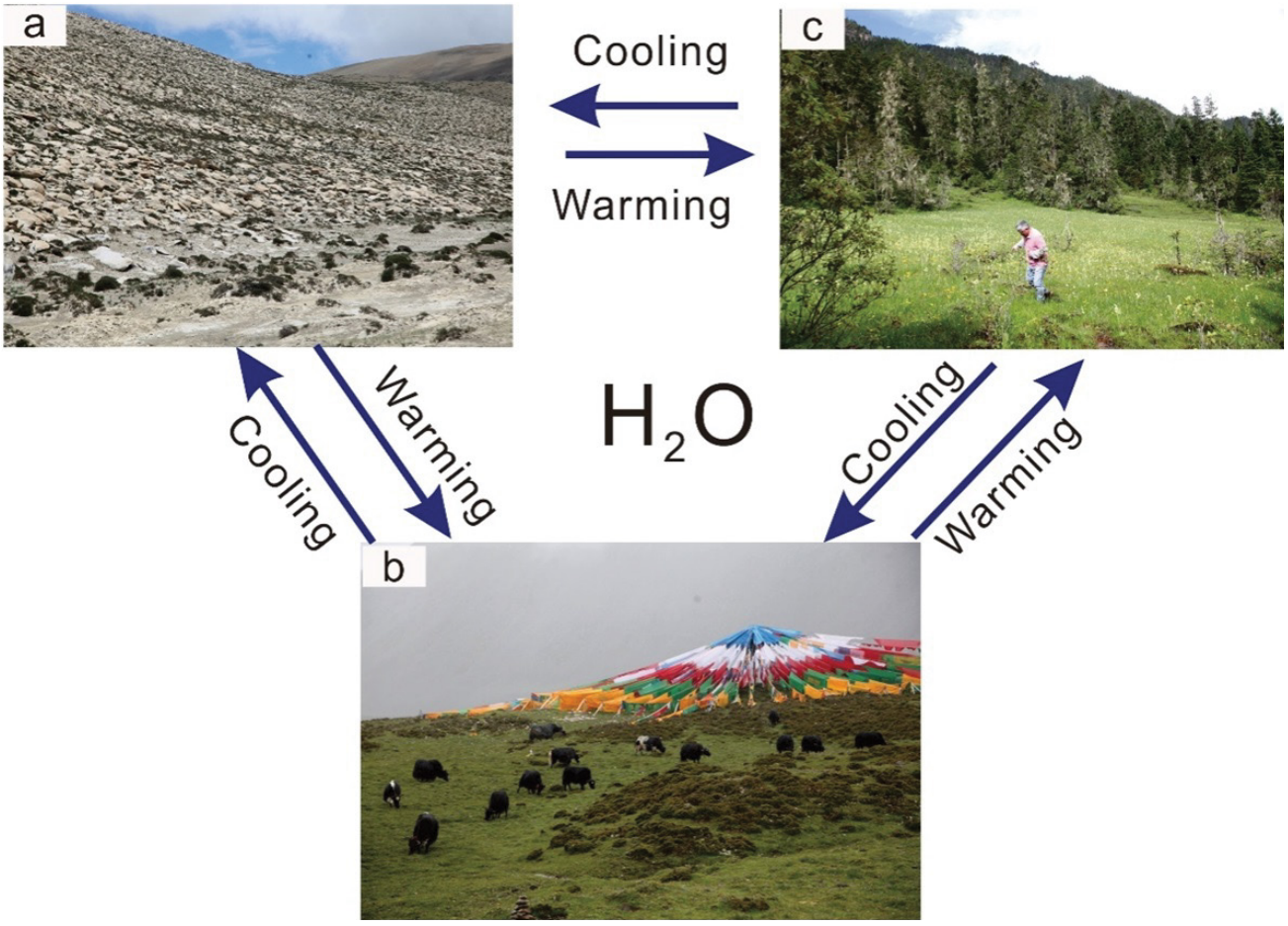

Figure 13: Schematic showing how the negative feedbacks between the growing Tibetan plateau and global climate change are working. When global atmospheric CO_2 concentrations are increased greatly, the surface average temperature is increased due to the enhanced greenhouse effect. And much freshwater is therefore towards Tibetan plateau [30-31,43]. The previously barren Tibetan regions (a) are quickly transformed to grass (b) and forest (c) wetlands, respectively, dependent on how much freshwater available, and vice versa. Subsequently the enhanced Tibetan geological carbon sink is working against the rise in global atmospheric CO_2 concentrations.

(e.g., Figure 2d). Therefore, the Tibetan geological carbon sink cannot be neglected in the near future. In addition, according to the method proposed by [31] firstly, within the southern Tibetan regions where the tectonics are the most active (Figure 1), approximately 30 and 100-150 tonnes of atmospheric CO_2 are estimated to be passively removed per year by the grass wetlands (e.g., Figures 5 and Figure 13b) and forest wetlands (e.g., Figure 4, Figure 10, Figure 11 and Figure 13c) per hectare, respectively. It should point out that the surface organic matters are not considered in this study, as some of them were rapidly buried by the active tectonics (e.g., Figure 10 and Figure 11) to easily yield double counting [31]. This means the model results here are underestimated slightly.

Although most Tibetan regions are barren lands because of freshwater-shortage (Figure 1, Figure 3 and Figure 13a), fossil studies [51,52] have further revealed that the barren Tibetan and its adjacent regions were fully covered by rain-forests or grass-wetlands during the previous warming periods. At that time, the entire Tibetan plateau was a greenly giant water-tower [30,31,43,51,52]. As demonstrated in the previous sections in detail, the carbon uptake by the tectonically active regions is strongly correlated with the surficial freshwater (Figure 2). These clearly indicate that the potential carbon uptake of the currently barren Tibetan regions where the tectonics are active (Figure 1, Figure 3 and Figure 13a) can be greatly improved rapidly by turning these tectonically active silicate lands poor in water (e.g., Figures 3 and Figure 13a)

Figure 14: Field photo showing Tibetan negative feedbacks. Yarlung Zangbo is a barrier lake now, leading to the enhancement of the Tibetan geological carbon sink to stop the rise of atmospheric CO_2 levels.

into artificial planting wetlands. Simple retaining dams constructed at the specific valleys can do this transformation rapidly. During summer, beneath the artificially planting wetlands within the tectonically active silicate regions, an extra huge amount of atmospheric CO_2 and freshwater are continuously sent to the much more depths through coupled the physiologically active plant roots and the active tectonics, subsequently chemically reacting with the deeply cracked silicates completely (e.g., Figure 7), regardless of whether there is heavy precipitation during summer. This implies that the currently negative correlation between the July's precipitation in southern Tibet and the annual growth rates (Figure 2) is probably replaced by a new one that the areas of the artificially planting wetlands within the most tectonically active silicate regions are negatively correlated with the annual growth rates of atmospheric CO_2 concentrations in the near future. During winter, massively newly-formed carbonates and organic matters are similarly deposited in the bottom of the artificially planting wetlands fast due to the strongly cold weather (e.g., Figure 9), also removing additionally huge amounts of atmospheric CO_2 directly. Moreover, physical weathering could be greatly diminished by the artificially planting wetlands, working against oxidization of the soil organic matter (e.g., Figure 2b). In addition, massively newly-formed carbonates and organic carbon in the artificial planting wetlands can be further buried in the thickened crust (e.g., Figure 10 and Figure 11). Therefore, the annual growth rates of the Tibetan atmospheric CO_2 concentrations will be largely diminished or even stopped completely by the vastly artificial planting wetlands within the most tectonically active silicate regions despite of currently massive anthropogenic emissions. Given that approximately 1 million square kilometers deserted regions, roughly 25% of the barren Tibetan and its adjacent regions (Figure 1), are rapidly transformed to artificially planting wetlands, net dozens of billion tonnes of atmospheric CO_2 could be directly removed per year by the Tibetan and its adjacent regions in the near future according to the relatively conservative estimations in this study.

The cost for the carbon uptake in this study is simply to construct the simple retaining dams at the specific valleys that can be used for several tens of years. These simple dams are mainly made up of local silicate rocks with minor cement and steel. Their sizes are generally 200 to 500 meters in length, 10 to 20 meters in height, and mean 200 meters in width. Excess water can easily across the simple dams to downstream. The total cost is approximately 1 million RBM for the constructure of one simple retaining dam that can be used for 30 years. The plateau internal is relatively flat so that a simple retaining dam can quickly transform 200 square kilometers barren deserts at least to artificial planting wetlands. As mentioned above in detail, approximately 30 tonnes of atmospheric CO_2 are removed per year per hectare by the grass wetlands (e.g., Figure 5 and Figure 13b). This means that it spends approximately 3 RMB to remove 60 tonnes atmospheric CO_2 per year. Therefore, the carbon uptake cost is less than 0.1 RMB/tonne/year here. Certainly, if local dominant species such as willows and pine trees are numerously planted in the artificial wetlands using the traditionally cheap approach, the carbon uptake cost will be even lower. Compared with the previously well-known approaches [7,8], this method is therefore the cheapest because of extremely low energy and infrastructure inputs every year. The global carbon neutrality is therefore achieved cheaply regardless of huge anthropogenic emissions in the near future. In addition, the mean global sea level hardly rises in the near future, as much freshwater is consecutively sent to Tibetan plateau and its adjacent inland regions from ocean [30,31,43], and thus cannot be back to ocean once again, partially due to these simply artificial retaining dams.

Conclusions

Although most Tibetan regions are barren deserts now, massively anthropogenic emissions are rapidly transformed to large amounts of secondary carbonates and organic carbon by a handful of Tibetan regions through the uniquely Tibetan geological carbon sink consisting of the enhanced subsurface silicate chemical weathering during summer and chemical sedimentation during winter, as well as the tectonic burial. The subsurface silicate chemical weathering is only working in the tectonically active silicate freshwater-enriched regions by coupled physiologically active plant roots and active tectonics. Whereas the chemical sedimentation occurs in the special setting of weak greenhouse effect with relatively high atmospheric CO_2 concentrations. The tectonic burial also occurs in the structurally unstable silicate regions rich in freshwater. Tibetan plateau boasts these unique features to become the only nascent carbon reservoir worldwide. The increasing in global atmospheric CO_2 concentrations is therefore regulated primarily by the Tibetan geological carbon sink. More importantly, the potential carbon uptake by the currently barren Tibetan regions where the tectonics are the most active could be greatly enhanced rapidly by turning these water-shortage silicate regions into artificially planting wetlands. The cheapest method for this transformation is simply to construct simple retaining dams at the specific valleys that can be used for several decades, as it requires extremely low energy and infrastructure inputs every year. If approximately 1 million square kilometers of Tibetan barren deserts are rapidly transformed to artificially planting wetlands within the tectonically active silicate regions, net dozens of gigatonnes of atmospheric CO_2 can be passively removed directly per year in the near future. The cost for the carbon uptake is as low as 0.1 RMB/tonne/year. Consequently, global carbon neutrality is easily achieved by the enhanced Tibetan geological carbon sink in the context of huge anthropogenic emissions.

Acknowledgments

We would really appreciate Dr. Yao Yang, Dr. Tingyuan Yuan, and Dr. Hongfei Liu for kind assistance during our field investigations.

References

1. Hubau W, Lewis SL, Phillips OL, Affum-Baffoe K, Beeckman H, et al. (2020) Asynchronous carbon sink saturation in African and Amazonian tropical forests. Nature 579: 80-87.

2. Gatti LV, Basso LS, Miller JB, Gloor M, Domingues LG, et al. (2021) Amazonia as a carbon source linked to deforestation and climate change. Nature 595: 388-393.

3. Wang YL, Wang X, Wang K, Chevallier F, Zhu D, et al. (2022) The size of the land carbon sink in China. Nature 603: E7-E9.

4. Friedlingstein P, Cox P, Betts R, Bopp L, Bloh WV, et al. (2006) Climate-carbon cycle feedback analysis: Results from the C^{4}MIP model intercomparison. Journal of Climate 19: 3337-3353.

5. Le Quere C, Rödenbeck C, Buitenhuis ET, Conway TJ, Langenfelds R, et al. (2007) Saturation of the Southern Ocean CO_2 sink due to recent climate change. Science 316: 1735-1738.

6. Ballantyne AP, Alden CB, Miller JB, Tans PP, White JWC (2012) Increase in observed net carbon dioxide uptake by land and oceans during the past 50 years. Nature 488: 70-73.

7. Hepburn C, Alden E, Beddington J, Carter EA, Fuss S, et al. (2019) The technological and economic prospects for CO_2 utilization and removal. Nature 575: 87-97.

8. Beerling DJ, Kantzas EP, Lomas MR, Wade P, Eufrasio RM, et al. (2020) Potential for large-scale CO_2 removal via enhanced rock weathering with croplands. Nature 583: 242-248.

9. Friedlingstein P, Jones MW, O'Sullivan M, Andrew RM, Bakker DEC, et al. (2021) Global carbon budget 2021. Earth System Science Data Discussions 1-191.

10. Ciais P, Tan J, Wang X, Roedenbeck C, Chevallier F, et al. (2019) Five decades of northern land carbon uptake revealed by the interhemispheric CO_2 gradient. Nature 568: 221-225.

11. Walker JCG, Hays PB, Kasting JF (1981) Negative feedback mechanism for the long-term stabilization of earth's surface temperature. Journal of Geophysical Research 86: 9776-9782.

12. Berner RA, Lasaga AC, Garrels RM (1983) The carbonate-silicate geochemical cycle and its effect on atmospheric carbon dioxide over the past 100 million years. American Journal of Science 283: 641-683.

13. Zeebe RE, Caldeira K (2008) Close mass balance of long-term carbon fluxes from ice-core CO_2 and ocean chemistry records. Nature Geoscience 1: 312-315.

14. Zachos JC, Dickens GR, Zeebe RE (2008) An early Cenozoic perspective on greenhouse warming and carbon-cycle dynamics. Nature 451: 279-283.

15. DeConto RM, Pollard D, Wilson PA, Pälike H, Lear CH, et al. (2008) Thresholds for Cenozoic bipolar glaciation. Nature 455: 652-656.

16. Pearson PN, Foster G L, Wade BS (2009) Atmospheric carbon dioxide through the Eocene-Oligocene climate transition. Nature 461: 1110-1113.

17. Pagani M, Huber M, Liu Z, Bohaty SM, Henderiks J, et al. (2011) The role of carbon dioxide during the onset of Antarctic glaciation. Science 204: 1261-1264.

18. Sundquist ET (1993) The global carbon dioxide budget. Science 259: 934-941.

19. Berner RA, Caldeira K (1997) The need for mass balance and feedback in the geochemical carbon cycle. Geology 25: 955-956.

20. Liu Y, Yang Z, Wang M (2007) History of zircon growth in a high-pressure granulite within the eastern Himalayan syntaxis, and tectonic implications. International Geology Review 49: 861-872.

21. Liu Y, Zhong DL (1997) Petrology of high-pressure granulites from the eastern Himalayan syntaxis. Journal of Metamorphic Geology 15: 451-466.

22. Liu Y, Siebel W, Massonne H-J, Xiao X (2007) Geochronological and petrological constraints for the tectonic evolution of the central Greater Himalayan Sequence in the Kharta area, southern Tibet. Journal of Geology 115: 215-230.

23. Zhang Z, Xiang H, Dong X, Li W, Ding H, et al. (2017) Oligocene HP metamorphism and anatexis of the Higher Himalayan Crystalline Sequence in Yadong region, east-central Himalaya. Gondwana Research 41: 173-187.

24. Arrhenius S (1896) On the influence of carbonic acid in the air upon the temperature on the ground. The Philosophical Magazine and Journal of Science 41: 237-279.

25. Chamberlin TC (1899) An attempt to frame a working hypothesis of the cause of glacial periods on an atmospheric basis. Journal of Geology 7: 667-685.

26. Raymo ME, Ruddiman WF (1992) Tectonic forcing of late Cenozoic climate. Nature 359: 117-122.

27. Edmond JM (1992) Himalayan tectonics, weathering processes and the strontium isotope record in marine limestone. Science 258: 1594-1597.

28. Liu Y, Berner Z, Massonne H-J, Zhong D (2006) Carbonatite-like dykes from the eastern Himalayan syntaxis: Geochemical, isotopic, and petrogenetic evidence for melting of metasedimentary carbonate rocks within the orogenic crust. Journal of Asian Earth Science 26: 105-120.

29. Liu Y (2013) Petrogenesis of carbonic dykes within southern Tibetan plateau, and climatic effects. Chinese Journal of Geology 48: 384-405.

30. Liu Y (2019) Effects of huge anthropogenic carbon emission: Inspiration from comprehensive investigations of Tibetan plateau. Geological Survey of China 6: 1-13.

31. Liu Y (2021) Analysis of global climate change in the next one hundred years. Geological Survey of China 8: 1-13.

32. Hartmann JA, West AJ, Renforth P, Köhler P, De La

Rocha CL, et al. (2013) Enhanced chemical weathering as a geoengineering strategy to reduce atmospheric carbon dioxide, supply nutrients, and mitigate ocean acidification. Reviews of Geophysics 51: 113-149.

33. Drake TW, Raymond PA, Spencer RG (2018) Terrestrial carbon inputs to inland waters: A current synthesis of estimates and uncertainty. Limnology and Oceanography Letters 3: 132-142.

34. Wang M, Shen ZK (2020) Present-day crustal deformation of continental China derived from GPS and its tectonic implications. JGR Solid Earth 125: e2019JB018774.

35. Wen YP, et al. (1997) A study of atmospheric CO_2 concentration variations and emission from the soil surface at MTWaliguan. Quarterly Journal of Applied Meteorology 8: 129-136.

36. Zhou LX, Tang J, Wen Y, Li J, Yan P, et al. (2003) The impact of local winds and long-range transport on the continuous carbon dioxide record at Mount Waliguan, China. Tellus B 55: 145-158.

37. Flechard CR, Neftel A, Jocher M, Ammann C, Leifeld J, et al. (2007) Temporal changes in soil pore space CO_2 concentration and storage under permanent grassland. Agriculture Forest Meteorology 142: 66-84.

38. Hashimoto S, Tanaka N, Kume T, Yoshifuji N, Hotta N, et al. (2007) Seasonality of vertically partitioned soil CO_2 production in temperate and tropical forest. Journal of Forest Research 12: 209-221.

39. Manning DAC, Renforth P (2013) Passive sequestration of atmospheric CO_2 through coupled plant-mineral reactions in urban soils. Environ Sci Technol 47: 135-141.

40. Dontsova K, Zaharescu D, Henderson W, Verghese S, Perdrial N, et al. (2014) Impact of organic carbon on weathering and chemical denudation of granular basalt. Geochimica Et Cosmochimica Acta 139: 508-526.

41. Riebe CS, Hahm WJ, Brantley SL (2017) Controls on deep critical zone architecture: A historical review and four testable hypotheses. Earth Surface Processes Landforms 42: 128-156.

42. Molnar P, England P, Martinod J (1993) Mantle dynamics, uplift of the Tibetan plateau, and the Indian monsoon. Reviews of Geophysics 31: 357-396.

43. Lehmkuhl F, Haselein F (2000) Quaternary paleoenvironmental change on the Tibetan plateau (western China and western Mongolia). Quaternary International 65-66: 121-145.

44. Ke LH, Song C, Wang J, Sheng Y, Ding X, et al. (2022) Constraining the contribution of glacier mass balance to the Tibetan lake growth in the early 21st century. Remote Sensing of Environment 268: 112779.

45. Chen C, Park T, Wang X, Piao S, Xu B, et al. (2019) China and India lead in greening of the world through land-use management. Nat Sustain 2: 122-129.

46. Zhu YK, Zhang T, Zhang Y, Qin S, Shao Y, et al. (2019) Responses of vegetation to climatic variations in the desert region of northern China. Catena175: 27-36.

47. Ding JZ, Chen L, Ji C, Hugelius G, Li Y, et al. (2017) Decadal soil carbon accumulation across Tibetan permafrost regions. Nature Geosciences 10: 420-424.

48. Wei D, Qi Y, Ma Y, Wang X, Ma W, et al. (2021) Plant uptake of CO_2 outpaces losses from permafrost and plant respiration on the Tibetan Plateau. Proc Natl Acad Sci USA 118: 2015283118.

49. Wang J, Feng L, Palmer PI, Liu Y, Fang S, et al. (2020) Large Chinese land carbon sink estimated from atmospheric carbon dioxide data. Nature 586: 720-723.

50. Yang D, Liu Y, Feng L, Wang J, Yao L, et al. (2021) The first global carbon dioxide flux map derived from TanSat measurements. Advances in Atmospheric Sciences 38: 1433-1443.

51. Huang J, Su T, Li S, Wu F, Deng T, et al. (2020) Pliocene flora and paleo environment of Zanda Basin, Tibet, China. Science China Earth Sciences 63: 212-223.

52. Qin F, Zhao Y, Cao X (2022) Biome reconstruction on the Tibetan Plateau since the Last Glacial Maximum using a machine learning method. Science China Earth Sciences 65: 536-552.

DOI: 10.35840/2631-5033/1864

Citation: Liu Y, He Y, Wang Y, Gao Z (2023) Rapid Stabilization on Global Atmospheric CO_2 Concentrations by Cheaply Enhanced Tibetan Geological Carbon Sink. Int J Earth Sci Geophys 9:064